HHS Public Access

Author manuscript

J Physiol. Author manuscript; available in PMC 2021 November 03.

Published in final edited form as:

J Physiol. 2020 December ; 598(24): 5639–5659. doi:10.1113/JP279909.

TRPV1 expressed throughout the arterial circulation regulates vasoconstriction and blood pressure

Thieu X. Phan[1,2], **Hoai T. Ton**[1,2], **Hajnalka Gulyás**[3], **Róbert Pórszász**[3], **Attila Tóth**[4], **Rebekah Russo**[5], **Matthew W. Kay**[5], **Niaz Sahibzada**[1], **Gerard P. Ahern**[1]

[1]Department of Pharmacology and Physiology, Georgetown University, Washington, DC, USA

[2]Department of Biology, Vinh University, Vinh, Vietnam

[3]Department of Pharmacology and Pharmacotherapy, Faculty of Medicine, University of Debrecen, Doctoral School of Pharmaceutical Sciences, Debrecen, Hungary

[4]Division of Clinical Physiology, Institute of Cardiology, Faculty of Medicine, University of Debrecen, Debrecen, Hungary

[5]Department of Biomedical Engineering, George Washington University, Washington, DC, USA

Abstract

The capsaicin receptor, TRPV1, is a key ion channel involved in inflammatory pain signalling. Although mainly studied in sensory nerves, there are reports of TRPV1 expression in isolated segments of the vasculature, but whether the channel localizes to vascular endothelium or smooth muscle is controversial and the distribution and functional roles of TRPV1 in arteries remain unknown. We mapped functional TRPV1 expression throughout the mouse arterial circulation. Analysis of reporter mouse lines TRPV1$^{PLAP\text{-}nlacZ}$ and TRPV1-Cre:tdTomato combined with Ca^{2+} imaging revealed specific localization of TRPV1 to smooth muscle of terminal arterioles in the heart, adipose tissue and skeletal muscle. Capsaicin evoked inward currents (current density ~10% of sensory neurons) and raised intracellular Ca^{2+} levels in arterial smooth muscle cells, constricted arterioles *ex vivo* and *in vivo* and increased systemic blood pressure in mice and rats. Further, capsaicin markedly and dose-dependently reduced coronary flow. Pharmacological and/or genetic disruption of TRPV1 abolished all these effects of capsaicin as well as vasoconstriction triggered by lysophosphatidic acid, a bioactive lipid generated by platelets and atherogenic

Corresponding author G. P. Ahern: Department of Pharmacology and Physiology, Georgetown University, Med-Dent Building SW401, 3900 Reservoir Rd, Washington, DC 20007, USA. gpa3@georgetown.edu.

Author contributions

T.P. designed and performed most of the experiments, analysed the data and helped write the article; G.A. conceived and designed experiments, performed electrophysiology and wrote the article; H.T. performed experiments; N.S. assisted with mouse BP measurements and helped write the article; H.G. and R.B. performed rat physiology and helped write the article. A.T. helped design experiments and helped write the article. R.R. and M.K. performed coronary flow experiments. All authors have read and approved the final version of this manuscript and agree to be accountable for all aspects of the work in ensuring that questions related to the accuracy or integrity of any part of the work are appropriately investigated and resolved. All persons designated as authors qualify for authorship, and all those who qualify for authorship are listed.

Competing interests

T.P. and G.A. are co-inventors of a provisional patent application related to technology presented in this article.

Supporting information

Additional supporting information may be found online in the Supporting Information section at the end of the article.

Statistical Summary Document

plaques. Notably, ablation of sensory nerves did not affect the responses to capsaicin revealing a vascular smooth muscle-restricted signalling mechanism. Moreover, unlike in sensory nerves, TRPV1 function in arteries was resistant to activity-induced desensitization. Thus, TRPV1 activation in vascular myocytes enables a persistent depolarizing current, leading to constriction of coronary, skeletal muscle and adipose arterioles and a sustained increase in systemic blood pressure.

Keywords

blood pressure; capsaicin; lysophosphatidic acid; TRPV1; vascular smooth muscle

Introduction

Transient receptor potential vanilloid 1 (TRPV1) is perhaps the best-studied member of the TRP ion channel family. The existence of highly specific and potent pharmacological agonists, including capsaicin, resiniferatoxin (Szallasi & Blumberg, 1999; Caterina & Julius, 2001) and spider toxins (Bohlen *et al*. 2010) along with recent electron cryomicroscopy (Cao *et al*. 2013; Liao *et al*. 2013; Gao *et al*. 2016) has enabled the inter-rogation of TRPV1 from the molecular to the whole animal level. The functional roles of TRPV1, however, have been appreciated for over 100 years owing to the ability of capsaicin to elicit pronounced pain responses (Szallasi & Blumberg, 1999; Caterina & Julius, 2001; Jancsó & Sántha, 2015). TRPV1 is highly expressed in a subset of sensory afferent nerves with cell bodies located in the dorsal root, trigeminal and nodose/jugular ganglia (Caterina *et al*. 1997). In many of these neurons TRPV1 acts as an integrator of noxious thermal and chemical stimuli including elevated heat, protons and lipid mediators (Tominaga *et al*. 1998; Caterina & Julius, 2001). These stimuli activate TRPV1, a non-selective cation channel with considerable Ca^{2+} permeability (Caterina *et al*. 1997), to depolarize the membrane and also to trigger the secretion of neuropeptides from nerve endings (Szallasi & Blumberg, 1999; Caterina & Julius, 2001). Accordingly, genetic or pharmacological inhibition of TRPV1 attenuates inflammatory pain (Caterina *et al*. 2000; Davis *et al*. 2000; Szallasi *et al*. 2007). Further, recent studies have revealed additional functions for TRPV1 as a transduction channel in both itch- and warm-temperature-coding neurons (Bautista *et al*. 2014; Yarmolinsky *et al*. 2016), thus indicating a broader role in somatosensory transmission.

Outside of sensory nerves, the expression and function of TRPV1 remain controversial. While there is considerable evidence for expression in select brain neurons (Cavanaugh *et al*. 2011), whether or not TRPV1 is functionally present in other tissues is less clear. Of note, several studies have described TRPV1 function in arterial smooth muscle cells of discrete tissues confirmed by measuring Ca^{2+} transients or vasoconstriction in response to capsaicin. Toth *et al*. described functional TRPV1 in arteriolar myocytes of gracilis muscle (Lizanecz *et al*. 2006; Kark *et al*. 2008; Czikora *et al*. 2012, 2013). Subsequently, Cavanaugh *et al*. using TRPV1 reporter mice described functional expression in smooth muscle cells of mouse cremaster muscle (Cavanaugh *et al*. 2011) while Phan *et al*. using genetic and pharmacological approaches reported sex dependent TRPV1 expression in smooth muscle of

bladder arterioles (Phan *et al.*, 2016). On the other hand, other studies have located TRPV1 in vascular endothelium (Bratz *et al.* 2008; Yang *et al.* 2010) and indicated that TRPV1 agonists dilate vessels to lower blood pressure. To further complicate matters, TRPV1 in sensory nerves can exert a neurogenic regulation of nearby blood vessels through the release of vasoactive peptides such as calcitonin gene related peptide (CGRP) or substance P. Indeed, local application of capsaicin to the skin is well known to cause a vasodilatation response accompanied by oedema (Baluk, 1997; Holzer, 1998).

Here, we exploited TRPV1 reporter mice combined with functional analyses to map TRPV1 expression throughout the arterial circulation. We show that TRPV1 is restricted to the smooth muscle of arterioles, notably in skeletal muscle, heart and adipose tissues. TRPV1 agonists, including inflammatory lipid mediators, evoke inward membrane currents in isolated vascular myocytes to persistently constrict arteries, decrease coronary flow and increase blood pressure. Furthermore, these effects are retained after the ablation of sensory nerves indicating an arteriole-mediated signalling mechanism. These data reveal a fundamental mechanism for transducing inflammatory stimuli into arterial constriction.

Methods

Ethical approval

All procedures were approved by Georgetown University, IACUC Protocol Numbers: 2016-1310 and 2018-0033; George Washington University, IACUC number A202, and University of Debrecen, Ethics Committee on Animal Research: 2/2013/DEMÁB and 4-1/2019/DEMÁB. All efforts were made to minimize the number and suffering of the animals used in this study. For CO_2 euthanasia animals were placed in a container with normal atmospheric gases and CO_2 inflow was initiated to produce ~30% volume displacement per minute.

Animals

Wistar and Sprague–Dawley rats (250–450 g) and C57Bl6 mice (25–30 g) were housed at 24–25°C and had *ad libitum* access to a standard laboratory chow and water.

Mouse lines

The TRPV1-Cre transgenic mouse line (donated by Dr Mark Hoon, NIH) was created using a BAC transgene containing the entire *Trpv1* gene/promoter (50 kbp of upstream DNA) and IRES-Cre-recombinase (Mishra *et al.* 2011). Importantly, *Cre* expression in this mouse faithfully corresponds with the expression of endogenous *Trpv1*. The TRPV1-Cre (hemizygous) mice were crossed with ai9 ROSA-stop-tdTomato mice (The Jackson Laboratory, Bar Harbor, ME, USA). The $TRPV1^{PLAP\text{-}nlacZ}$ mice (Jackson Laboratory) were developed by Allan Bausbaum and colleagues (UCSF) to express human placental alkaline phosphatase (PLAP) and nuclear lacZ under the control of the *TRPV1* promoter (Cavanaugh *et al.* 2011). The targeting construct contains an IRES-PLAP-IRES-nlacZ cassette immediately 3′ of the TRPV1 stop codon, which permits the transcription and translation of PLAP and nlacZ in cells expressing TRPV1 without disrupting the *Trpv1* coding region. TRPV1-null mice were purchased from The Jackson Laboratory.

TRPV1-Cre:ChR2/tdTomato mice were generated by crossing TRPV1-Cre mice with ChR2/tdTomato mice (The Jackson Laboratory).

X-gal staining

TRPV1$^{PLAP\text{-}nlacZ}$ mice were anaesthetized with isoflurane (4% in 100% O_2), and euthanized by perfused the heart using phosphate-buffered saline (PBS; 0.1 M, pH 7.3) followed by ice-cold 2–4% buffered paraformaldehyde. Whole skinned mice, brains, hearts and trunk arteries were dissected and postfixed in 2–4% buffered paraformaldehyde on ice for 90 min, after which they were washed in PBS (containing 5 mM EGTA and 2 mM $MgCl_2$) on ice and stained in X-gal solution (containing 1 mg/ml X-gal, 5 mM $K_3Fe(CN)_6$, 5 mM $K_4Fe(CN)_6$, 0.01% deoxycholate and 2 mM $MgCl_2$ in PBS) at 37°C overnight. nLacZ staining was imaged *in situ*, in heart sections (120–150 μm thick) and isolated arteries. To calculate the density of the signal, defined arteries and arterioles were isolated from TRPV1$^{PLAP\text{-}nlacZ}$ and wild-type mice, stained and photographed in parallel. Densitometry was performed with ImageJ to yield density in arbitrary units (normalized to the wild-type signal). To map arterial/arteriole TRPV1 expression we compared the density of X-gal staining in main trunk arteries and tributaries, heart and brain. The distribution of intensities revealed five broad peaks (a baseline and four positive peaks, see for example Fig. 6B) that were colour-coded from zero (dark blue) to a maximum (red).

TRPV1 mRNA analysis

Mice were anaesthetized with isoflurane (4% in 100% O_2) and euthanized by perfusing the heart with ice-cold PBS (0.1 M, pH 7.3). Dorsal root ganglia (L4, L5), brachial and radial branch arteries were isolated. RNA was extracted and purified using the RNAqueous Micro Kit (Thermo Fisher Scientific, Waltham, MA, USA). Quantitative PCR analysis was performed with TaqMan Fast Advance Mastermix (Thermo Fisher Scientific), with proprietary *TRPV1* gene probes labelled by FAM (Mm01246302_m1 from Thermo Fisher Scientific) and *GAPDH* control gene expression probe labelled by VIC (Mm99999915_g1). Thermal cycling of the PCR reaction was as follows: 50°C for 2 min, 95°C for 3 min, 50 cycles at 95°C for 15 s and 58°C for 1 min. Data were collected at the end of the 58°C anneal/extend step. Data were analysed after the reaction using the Auto Ct function of the SDS 1.4 software (Thermo Fisher Scientific), and the reactions were considered to have passed quality control if the standard deviation of the C_t values were less than 0.5. The comparative C_t method was used to present gene expression of *TRPV1* relative to *GAPDH*.

Immunostaining and $DiOC_{18}$ labelling

Mice were anaesthetized with isoflurane (4% in 100% O_2) and euthanized by perfusing the heart with PBS (0.1 M, pH 7.3) followed by ice-cold 2–4% paraformaldehyde (in PBS). For endothelial labelling, mice were perfused with the green fluorescent dye 3,3′-dioctadecyloxacarbocyanine perchlorate ($DiOC18_3$; Sigma-Aldrich). $DiOC18_3$ stock was prepared at 3 mg/ml in ethanol and diluted 50× in PBS. Arteries were isolated, fixed in 4% buffered paraformaldehyde for 1.5 h and stored in 30% sucrose overnight. Arteries were then embedded in low-temperature agarose before sectioning (15 μm). Sections were stained with primary anti-bodies, anti-LacZ (1:100, The Developmental Studies Hybridoma Bank, University of Iowa, Iowa City, IA, USA) and anti-CD31-FITC (1:50, BioLegend, San Diego,

CA, USA) followed by a goat anti-mouse IgG-AlexaFluor 555 secondary antibody (1:300, Thermo Fisher Scientific). Images were acquired by confocal microscopy.

Sensory nerve culture

Dorsal root and nodose ganglia were obtained from adult mice C57BL/6J) euthanized by exposure to a rising concentration of CO_2 followed by decapitation. Ganglia were trimmed, digested with collagenase, and cultured in Neurobasal plus 2% B-27 medium (Thermo Fisher Scientific), 0.1% L-glutamine, and 1% penicillin–streptomycin on poly-D-lysine-coated glass coverslips at 37°C in 5% CO_2. Neurons were used within 24–36 h of culture.

Arterial smooth muscle cell isolation

Adult mice (C57BL/6J) were euthanized by exposure to a rising concentration of CO_2 followed by decapitation. Radial artery branch (artery no. 18, see Fig. 6G) and cerebellar branch (cerebral artery no. 3, see Fig. 6G) was washed in Mg^{2+}-based physiological saline solution (Mg-PSS) containing 5 mM KCl, 140 mM NaCl, 2 mM $MgCl_2$, 10 mM HEPES and 10 mM glucose (pH 7.3). Arteries were initially digested in papain (0.6 mg/ml) (Worthington Biochemical Corp., Lakewood, NJ, USA) and dithioerythritol (1 mg/ml) in Mg-PSS at 37°C for 15 min, followed by a 15-min incubation at 37°C in type II collagenase (1.0 mg/ml) (Worthington) in Mg-PSS. The digested arteries were washed 3 times in ice-cold Mg-PSS solution and incubated on ice for 30 min. After this incubation period, vessels were triturated to liberate smooth muscle cells and stored in ice-cold Mg-PSS before use. Smooth muscle cells adhered loosely to glass coverslips and were studied within 6 h of isolation.

Ca^2 imaging

Arterial smooth muscle (ASM) cells and arteries were respectively loaded with 5 μM and 10 μM Fluo-4-AM (Thermo Fisher Scientific) in a buffer solution containing 140 mM NaCl, 4 mM KCl, 1 mM $MgCl_2$, 1.2 mM $CaCl_2$, 10 mM HEPES and 5 mM glucose (pH 7.3). Temperature was maintained at 32–33°C using a heated microscope stage (Tokai Hit, Fujinomiya, Japan). Bath temperature was verified by a thermistor probe (Warner Instruments, Hamden, CT, USA). ASM cells and arteries were imaged with ×10 and ×20 objectives using a Nikon TE2000 microscope with an excitation filter of 480 ± 15 nm and an emission filter of 535 ± 25 nm. The images were captured by a Retiga 3000 digital camera (QImaging, Surrey, BC, Canada) and analysis was performed offline using ImageJ.

Electrophysiology

Whole-cell patch-clamp recordings were performed using an EPC8 amplifier (HEKA Instruments, Holliston, MA, USA). Pipette resistances were in the range 3–4 MΩ and the current signal was low-pass filtered at 1–3 kHz and sampled at 4 kHz. The bath solution was the same as described for Ca^{2+} imaging (290 mosmol l^{-1}). The pipette solution contained: 140 mM CsCl, 10 mM HEPES, 5 mM EGTA, and 1 mM $MgCl_2$, pH 7.3. In some experiments the EGTA concentration was reduced to 0.2 mM.

Ex vivo artery physiology

Mice and rats were euthanized by exposure to a rising concentration of CO_2 followed by decapitation. Skeletal muscle arteries (radial artery branch, artery no. 18, subscapular branch artery no. 14, gracilis artery no. 29, and cerebellar branch, cerebral artery no. 3, see Fig. 6G) were isolated and cannulated with glass micropipettes, and secured with monofilament threads. In some experiments arteries were denuded of endothelium by passing 1 ml of air followed by 1 ml of PSS through the lumen. Effective removal of the endothelium was confirmed by the absence of dilatation of the arteries to ACh. The pipette and bathing PSS solution (containing in mM: 125 NaCl, 3 KCl, 26 $NaHCO_3$, 1.25 NaH_2PO_4, 1 $MgCl_2$, 4 D-glucose and 2 $CaCl_2$) was aerated with a gas mixture consisting of 95% O_2–5% CO_2 to maintain pH (pH 7.4). To induce maximal dilatation, arteries were perfused with a PSS solution containing 0 $CaCl_2$, 0.4 mM EGTA and 100 μM sodium nitroprusside. Arterioles were mounted in a single vessel chamber (Living Systems Instrumentation, St Albans City, VT, USA) and placed on a heated imaging stage (Tokai Hit) to maintain bath temperature between 34 and 35°C, while intraluminal pressure was maintained by a Pressure Control Station (Stratagene, San Diego, CA, USA) at 60 mmHg. Arteries were viewed with a ×10 objective using a Nikon TE2000 microscope and recorded by a digital camera (Retiga 3000, QImaging). The arteriole diameter was measured at several locations along each arteriole using the NIH ImageJ software's edge-detection plug-in (Diameter) (Fischer *et al.* 2010). The software automatically detects the distance between edges (by resampling a total of 5 times from adjacent pixels) yielding a continuous read-out ±SD of a vessel's diameter.

Coronary arterioles were visualized in sagittal tissues slices (120–150 μm) prepared from the hearts of TRPV1-Cre:tdTomato mice. Slices were perfused at room temperature with the same PSS solution as for pressurized arteries.

Intravital imaging

Intravital imaging was performed in radial artery branches (about 60 μm in diameter, artery no. 18 in Fig 6G). Mice were restrained by grasping the skin at the nape of the neck and anaesthetized with urethane (1.2 g/kg, I.P.). The adequacy of anaesthesia was confirmed by the absence of pedal and corneal reflexes. The forelimb was shaved and an incision was made. The skin and underlying muscle tissue were reflected to expose the brachial–radial artery junction. Both in WT and TRPV1-null mice, the arteries were visualized with a Zeiss stereomicroscope and illuminated with a low power blue light (using a standard green fluorescent protein filter cube) exploiting the differential auto-fluorescence between tissue and blood. In TRPV1-Cre:ChR2/tdTomato mice, arteries were visualized with low power visible irradiation and stimulated with blue light. The exposed arteries were locally perfused (using a 250 μm cannula connected to a valve-controlled gravity-fed perfusion system) with preheated buffer described for Ca^{2+} imaging. The surface tissue temperature (34–35°C) was measured via a thermistor (Warner Instruments) that was positioned next to the artery. Arteries were challenged with buffer without Ca^{2+} and with 1 mM EGTA to measure the passive diameter. The arteriole diameter was measured using ImageJ as described above for the *ex vivo* vessels. After the recordings, the mice were euthanized by CO_2 (gas cylinder)/ decapitation.

Coronary flow measurements

Sprague–Dawley rats (male, 300–350 g) were placed in a deep surgical plane of anaesthesia by isoflurane inhalation (4% in 100% O_2), confirmed by lack of pedal reflex. The heart was then exposed via thoracotomy, quickly excised and rinsed in a bath of ice-cold perfusate. The aorta was rapidly cannulated then flushed with 500 units of heparin mixed with the perfusate that contained (in mM): 118 NaCl, 4.7 KCl, 1.25 $CaCl_2$, 0.57 $MgSO_4$, 1.17 KH_2PO_4, 25 $NaHCO_3$ and 6 glucose. Hearts were then transferred to a retrograde perfusion system that delivered oxygenated (gassed with 95% O_2–5% CO_2) perfusate to the aorta at constant pressure (70 mmHg) and 37 ± 1°C. Coronary flow was measured using a tubing flowsensor (Transonic Systems, Ithaca, NY, USA) placed above the aortic cannula and was continuously acquired with the ECG using a PowerLab system (ADInstruments, Sydney, Australia). Bolus injections of capsaicin were administered in-line above the aorta. 4-(3-Chloro-2-pyridinyl)-*N*-[4-(1,1-dimethylethyl)phenyl]-1-piperazinecarboxamide (BCTC) was added to the perfusate reservoir. Data were analysed off-line and the integral of coronary flow was calculated between the time of injection and the onset of the hyperaemia response.

Sensory nerve ablation

Neonate $TRPV1^{PLAP\text{-}nlacZ}$ mice were anaesthetized briefly (5 min) with isoflurane (4–5% in 100% O_2) and treated with resiniferatoxin (50 ug/kg S.C.) at postnatal days 2 and 5. Animals were allowed to recover in a warm environment (30°C, 2 h) to minimize any hypothermic effects. This dose of resiniferatoxin causes profound sensory nerve desensitization/block and mice exhibited no outward signs of distress in recovery, and there was no disruption to dam–pup interactions. At 8–12 weeks, mice were either euthanized for tissue collection, or used for blood pressure (BP) measurements and immediately euthanized by exposure to a rising concentration of CO_2 followed by decapitation. Sensory nerve ablation was confirmed by nuclear LacZ staining of DRG ganglia.

New-born rats (postnatal day 14) were anaesthetized by isoflurane (AErrane, Baxter, Deerfield, IL, USA), nitrous oxide (Linde, Dublin, Ireland) and oxygen (Linde, Dublin, Ireland) mixture (70% N_2O and 30% O_2 and 0.8% isoflurane). Then they were pre-treated with a mixture of aminophylline (Diaphylline, Richter, Budapest, Hungary, dose 19.2 mg/kg), Bricanyl (terbutaline, Astra Zeneca, Budapest, Hungary, dose 0.2 mg/kg), atropine (Atropinum sulfuricum, Egis, Budapest, Hungary dose 0.2 mg/kg) in a volume of 0.1 ml/100 g I.P. This bronchodilator mixture reduced the animal loss because of systemic high dose of capsaicin administration. Ten minutes later animals were injected with capsaicin (subcutaneously). After the injection of capsaicin, the animals were placed in a cotton-filled cage for the recovery period and an infrared heating lamp was used to keep the environmental temperature around 30°C. The rat pups were placed back in their original cage after total recovery from anaesthesia.

The procedure was repeated for a total of five consecutive days. The total dose of capsaicin was 300 mg/kg, administered on a dose schedule of 10, 20, 50, 100 and 120 mg/kg on days 1–5, respectively. Rats were then kept in the animal facility for 10 weeks until experiments were performed. Animals were euthanized by exposure to a rising concentration of CO_2 followed by decapitation.

Measurement of capsaicin-evoked sensory irritation

One drop (10 μl) of capsaicin solution (50 μg/ml in physiological saline) was put into the right or left conjunctiva of the rat, in a random order. The number of eye wipes was counted during 60 s. Capsaicin instilled into the conjunctival sac of a naive animal causes transient irritation, which lasts a maximum of ~1 min. During only this period the animals respond with eye wipes. After 1 min, no behaviour induced by any irritation can be observed. The formerly desensitized animals do not show any kind of irritation at all and the eye wiping behaviour is completely absent. Each animal was used for one test only. In the systemic blood pressure measurement experiments, we only used animals that were desensitized and did not respond to the capsaicin eye challenge. The others were euthanized by 250 mg/kg thiopenthal I.P.

Systemic blood pressure recording

The experiments were performed in anaesthetized mice (urethane 1.2–1.5 g/kg I.P.) and rats (thiopental 50 mg/kg I.P.; supplemented by 5 mg/kg I.V. if needed). After anaesthesia, mice or rats underwent cannulation of the carotid artery and jugular vein as follows.

Surgical preparation in the mouse

After the depth of anaesthesia was confirmed by lack of pedal and corneal reflexes, mice were intubated via the trachea after tracheotomy to maintain an open airway and to institute artificial respiration when necessary. Next, the left carotid artery and the right jugular vein were cannulated with a Millar (Houston, TX, USA) catheter (1F SPR-1000) and polyethylene tubing (PE-10), respectively, for monitoring arterial blood pressure and for systemic (intravenous) infusion of drugs. To monitor heart rate, a three-point needle electrode assembly representing Lead II of the electrocardiogram (ECG) was attached subcutaneously to the right and left forelimbs along with a reference electrode to the left hindlimb. Both the Millar catheter and the ECG assembly were coupled to a PowerLab data acquisition system (ADInstruments). Before vessel cannulation, the adjacent left cervical vagus was carefully isolated from the left carotid artery. Body temperature was monitored by a digital rectal thermometer and maintained at 37 ± 1°C with an infrared heat lamp. After the study, mice were euthanized by exposure to a rising concentration of CO_2 followed by decapitation.

Conscious blood pressure recordings

Resiniferatoxin (RTX)-treated mice (8–12 weeks) were anaesthetized with isoflurane (2–4%) and surgically implanted with in-dwelling jugular catheters (Instech Laboratories, Plymouth Meeting, PA, USA). The adequacy of anaesthesia was confirmed by the absence of pedal and corneal reflexes. Post-surgically mice were administered carprofen (one dose of 5 mg/kg S.C.) and placed in a cotton-filled cage until ambulatory. After 72 h, the animals were prepared for BP recording. BP was measured by tail-cuff plethysmography (Coda6, Kent Scientific, Torrington, CT, USA) performed before and immediately after the infusion of drugs. At the end of the study, the mice were euthanized by exposure to a rising concentration of CO_2 followed by decapitation.

Surgical preparation in the rat

Before the commencement of surgical interventions, the depth of anaesthesia was checked by squeezing the tip of the rat's tail. If no response to this challenge was observed, the animal was fixed to a plastic foil-covered polystyrene plate by strings and tapes. The animal was placed in a supine position and the collar region was shaved by a razor. A midline incision was made to expose the trachea, carotid arteries and jugular vein. Similar to the mouse, following intubation of the trachea, the left carotid artery and jugular vein were cannulated with a polyethylene tubing (PE50) to monitor blood pressure and infuse drugs, respectively. Blood pressure (and ECG) was continuously recorded via a pressure transducer connected to the Haemosys hemodynamic system (Experimetria, Budapest, Hungary). The ECG was recorded from the extremities of the animal using hypodermic metal needles inserted subcutaneously as per the Einthoven method (I, II, III leads). As in the mouse, heart rate was determined from lead II of the ECG recordings, and body core temperature was maintained at 37 ± 1°C with a temperature-controlled infrared heating lamp. During the experiment, the depth of anaesthesia was checked regularly and if necessary was supplemented by an intravenous dose of 5 mg/kg thiopental. After the study, the animals were euthanized by exposure to a rising concentration of CO_2 followed by decapitation.

Drug administration

Intravenous infusion of drugs was initiated only when a stable baseline of blood pressure and heart rate was present. This was also the case when drugs were re-administered. Final drug solutions contained: capsaicin (saline with 0.4% ethanol), lysophosphatidic acid (LPA; saline with 0.6% ethanol).

Chemicals

Capsaicin, resiniferatoxin and BCTC were purchased from Tocris Bioscience (Minneapolis, MN, USA) or Adooq Bioscience (Irvine, CA, USA) and stock solutions were prepared in ethanol at 1 M and 100 mM, respectively. LPA C18:1 was purchased from Cayman Chemical (Ann Arbor, MI, USA). Unless otherwise indicated, all other chemicals were obtained from Sigma-Aldrich.

Statistical analysis

Data were analysed using Prism (GraphPad Software, La Jolla, CA, USA) and are expressed as means ± SD. Unless otherwise stated, statistical significance was evaluated using Student's *t* test and one-way ANOVA with treatment interactions assessed by Tukey's *post hoc* multiple comparisons test. A P value of <0.05 was considered statistically significant.

Results

TRPV1 in arteries is restricted to vascular smooth muscle

Previous studies using antibodies have described TRPV1 expression in both vascular smooth muscle (Lizanecz *et al.* 2006; Toth *et al.* 2014) and endothelium (Bratz *et al.* 2008; Yang *et al.* 2010). However, the potential for non-specific labelling, well demonstrated for TRPV1 antibodies (Toth *et al.* 2014; Sand *et al.* 2015), limits the interpretation of these data. To

better define arterial expression of TRPV1 we exploited two validated mouse reporter lines. The first, TRPV1-Cre:tdTomato (Mishra *et al.* 2011), generates a very sensitive fate map of TRPV1 expression. The second, $TRPV1^{PLAP\text{-}nlacZ}$ (Cavanaugh *et al.* 2011), generates expression of human placental alkaline phosphatase (PLAP) and nuclear β-galactosidase (nLacZ) under the control of the endogenous *Trpv1* promoter. Analysis of arterioles from TRPV1-Cre:tdTomato mice revealed robust tomato fluorescence in vascular smooth muscle that did not extend to the endothelium labelled with DioC18 (green, Fig. 1A). Similarly, co-labelling arteries from $TRPV1^{PLAP\text{-}nlacZ}$ mice with antibodies to LacZ and the endothelial marker, CD31, revealed distinct, non-overlapping staining of smooth muscle and endothelium (Fig. 1B–E). In total, we examined co-labelling in eight mice and failed to detect any TRPV1 endothelial labelling. Thus, TRPV1 expression in murine arteries appears to be restricted to vascular smooth muscle.

Arteriolar TRPV1 is prominent in skeletal muscle, heart and adipose tissues

Next, we mapped TRPV1 expression through the arterial network of the mouse (n = 36 reporter mice). Remarkably, we found that TRPV1 was highly enriched in small (resistance) arterioles (<150 μm diameter) of the heart, skeletal muscle and adipose tissues (Fig. 2). In the heart, large epicardial arteries were devoid of TRPV1 expression but strong tdTomato fluorescence (Fig. 2A and B) and nLacZ staining (Fig. 2C and D) emerged as these arteries penetrated and branched in the myocardial wall. Similarly, TRPV1 expression erupted as forelimb arteries branched to supply skeletal muscle (Fig. 2E–H). Indeed, analysis of skeletal muscle in isolated tissue (Fig. 2I–L) or in whole animal preparations (Fig. 3) revealed an abundant network of TRPV1-expressing arteries. Note that the LacZ reporter is nuclear restricted and therefore the abundant staining in skeletal muscle (Fig. 3) excludes labelling of sensory nerve fibres. Additionally, LacZ prominently stained vascular smooth muscle of arteries in both white and brown adipose tissue (Fig. 2M–R). In whole animal preparations, marked labelling was apparent in arterioles supplying the interscapular fat (Fig. 3E). We also detected TRPV1 reporter expression in select parts of the cerebral circulation, including prominent labelling in the hypophyseal portal arteries and small-diameter branches of the basilar arteries (data not shown), and in very small mesenteric arteries (<50 μm, Fig. 4I–L). In addition, microvessels or ‘vasa vasorum’ supplying the wall of large arteries highly expressed TRPV1 (Fig. 4B). In contrast, we found very limited TRPV1 expression in the aorta and large trunk arteries (Fig. 4A–E) or arteries of other tissues examined, including skin, lung, kidney and liver (data not shown). In total, we analysed 30 male and six female reporter (TRPV1-LacZ) mice and no obvious sex differences were noted in the expression pattern.

Next, to confirm that TRPV1 is functionally expressed, we performed Ca^{2+} imaging in isolated arterioles and arteriolar smooth muscle (ASM) cells. The TRPV1-specific agonist, capsaicin, increased Ca^{2+} signalling in a subset of arterioles isolated from wild-type mice, whereas we observed no responses in the same arterioles from TRPV1-null mice (P = 0.00013, Fig. 5A–D). Furthermore, capsaicin sensitivity in ASM cells isolated from TRPV1-Cre:tdTomato mice was restricted to Tomato-positive cells (Fig. 5E and F), and was abolished after removing external Ca^{2+} indicating an essential role for Ca^{2+} entry (Fig. 5G). Finally, capsaicin (5 μM) evoked inward currents in voltage-clamped ASM cells isolated

from skeletal muscle arterioles (mean 8.7 ± 2.7 pA/pF, $n = 9$) that were fully prevented by the TRPV1 antagonist, BCTC ($P = 0.0013$, Fig. 5H and I). The peak current density was ~11% of that observed in cultured sensory neurons (Fig. 5I).

To confirm the fidelity of the TRPV1 reporter, we compared both TRPV1 mRNA levels and the capsaicin sensitivity of arteries with differential reporter expression (Fig. 6). Analysis of arteries at different positions along the axial-brachial trunk and branches (Fig. 6A) revealed that TRPV1 LacZ reporter expression was inversely proportional to the arterial diameter (Fig. 6B). Similarly, quantitative PCR showed that TRPV1 mRNA levels were greater in smaller diameter arterioles peaking at ~13% of DRG levels (Fig. 6C). Furthermore, results of Ca^{2+} imaging showed that the number of ASM cells responding to capsaicin (Fig. 6D and E) and the magnitude of the Ca^{2+} signal (Fig. 6D and F) increased in proportion to the TRPV1 reporter signal (nLacZ staining density). Based on TRPV1 reporter analysis, validated by functional imaging, we constructed a heat map of TRPV1 expression in the mouse arterial system (Fig. 6G and Table 1). This map highlights the hierarchical distribution of TRPV1 becoming abundant in small-diameter resistance arterioles of skeletal muscle and heart (adipose is not represented here).

TRPV1 constricts arterioles *ex vivo* and *in vivo*

To identify a physiological role for vascular TRPV1, we studied contractility in isolated, pressurized arteries. Capsaicin (1 μM) constricted (by ~80–85%, $P = 3 \times 10^{-8}$) arterioles isolated from wild-type mice without affecting vessels from TRPV1-null mice (Fig. 7A and B). Analysis of the response to varying capsaicin concentrations revealed a half-maximal effect at ~150 nM that was unaffected by removing the vascular endothelium (Fig. 7C) consistent with capsaicin selectively acting on arterial smooth muscle. To measure the *in vivo* functionality of arterial TRPV1, we performed intravital imaging of radial muscle branch arteries. Local administration of capsaicin constricted these arteries (by ~90%, $P = 1 \times 10^{-8}$) without affecting nearby veins, or arteries in TRPV1-null mice (Fig. 7D and E).

Finally, we tested the relative contribution of Ca^{2+} entry via TRPV1 or voltage-gated channels. Indeed, the L-type voltage-gated Ca^{2+} channel (Cav1.2) is a major determinant of resting tone in arterioles. We found that nifedipine (3 μM) almost completely relaxed skeletal muscle arterioles *in vivo*, but only partly (~30%, $P = 0.027$) inhibited the constriction evoked by a saturating concentration of capsaicin (Fig. 7F), suggesting that Ca^{2+} influx through fully activated TRPV1 channels is sufficient to constrict arteries, while L-type channels amplify the magnitude of the constriction. Figure 7G, summarizes the signalling pathways for TRPV1-mediated vasoconstriction: Ca^{2+} entry via TRPV1 and depolarization-evoked Ca^{2+} entry via Cav1.2. It should be noted that, Ca^{2+} entry via either of these pathways may trigger additional Ca^{2+} release from intracellular stores.

TRPV1 constricts coronary arterioles and decreases coronary flow

The striking expression of TRPV1 in the coronary vasculature (Fig. 2A–D) prompted us to explore functional effects of TRPV1 activation. Analysis of heart sections from TRPV1 reporter mice (Fig. 8A and B) revealed that TRPV1 expression was restricted to small arterioles that branch from the large coronary arteries (yellow arrowheads). Application

of capsaicin 1 μM to sagittal slice preparations ~150 μm) of living heart tissue (TRPV1-Cre:tdTomato mice) constricted these small arterioles by up to 60%, visualized by tdTomato fluorescence, and the magnitude of the response was inversely proportional to the artery diameter (Fig. 8C–E). Although these studies were performed in non-pressurized arteries, and the magnitude of the responses compared with pressurized arteries should be interpreted cautiously, they non-etheless demonstrate capsaicin sensitivity in these vessels consistent with the level of TRPV1 expression. Next, we examined a role for TRPV1 in the regulation of coronary flow in isolated hearts. In these experiments, we used rats as we found that capsaicin evoked equivalent vasoconstriction in both rodent species (see Fig. 7B and C). Administration of capsaicin (by 10 s in-line infusion) decreased coronary flow in a dose-dependent manner by up to 30 ml/min ($P = 2.5 \times 10^{-4}$, Fig. 8F–H). This decrease was followed by rebound hyperaemia (Fig. 8F). The decrease in flow occurred without a change in heart rate (6 μg capsaicin, $P = 0.983$, Fig. 8H) and was fully prevented by pre-treatment with BCTC ($P = 0.957$, Fig. 8F and G).

Arterial TRPV1 regulates systemic blood pressure

The extensive expression in arteriolar smooth muscle makes TRPV1 well situated to influence systemic blood pressure (BP). We therefore tested whether TRPV1 agonists would alter BP as predicted by their profound vasoconstrictive effects detailed above. Indeed, intravenous administration of capsaicin to anaesthetized mice markedly increased BP by ~45 mmHg ($P = 1 \times 10^{-9}$), while TRPV1-null mice exhibited no responses to capsaicin demonstrating a selective action at TRPV1 (Fig. 9A and B). We observed equivalent BP responses to capsaicin in conscious mice ($P = 2.5 \times 10^{-4}$, Fig. 9K), thus ruling out side effects of anaesthesia. Similarly, in rats, capsaicin produced a dose-dependent increase in BP with an approximate 60 mmHg rise in systolic and diastolic blood pressure observed at the highest dose tested ($P = 1.5 \times 10^{-6}$, Fig. 9D). The peak responses to capsaicin occurred without any significant changes in heart rate (Fig. 9C and E) demonstrating a predominant effect on peripheral vascular resistance.

Although the pressor response to capsaicin is consistent with actions at arterial TRPV1, these data do not exclude a contribution of TRPV1 in perivascular sensory nerves. TRPV1-expressing nerves may affect blood flow by releasing vasoactive peptides such as CGRP (Zygmunt *et al.* 1999) or neurokinins (Baluk, 1997; Holzer, 1998). Therefore, to discriminate between an arterial and a neurogenic locus of TRPV1 signalling, we performed selective ablation of TRPV1-expressing sensory nerves. Resiniferatoxin (RTX) or capsaicin administered systemically to neonates causes permanent deletion of most TRPV1-positive sensory nerves (Jancsó *et al.* 1977; Szallasi & Blumberg, 1992). In contrast, TRPV1-expressing arterial smooth muscle exhibits full functional recovery from this treatment (Czikora *et al.* 2013). Indeed, 8 weeks following RTX administration to TRPV1-nLacZ mice, we observed an almost complete loss of nLacZ staining in DRG neurons, whereas arterial staining was unaffected (Fig. 9F). Similarly, treating neonatal rats with capsaicin abolished subsequent nocifensive responses (eye-wipes) to capsaicin ($P = 1 \times 10^{-9}$, Fig. 9G) consistent with ablation of TRPV1-expressing sensory neurons. Notably, administration of capsaicin to these sensory-nerve ablated mice and rats evoked pressor responses similar to

untreated controls (Fig. 9H–J). Thus, we conclude that sensory nerves play little to no role in the capsaicin-evoked BP rise.

In previous studies, capsaicin was shown to elicit a cardiopulmonary Bezold–Jarisch reflex consisting of a transient drop in BP, bradycardia and apnoea (Szolcsanyi *et al.* 1990). Indeed, we observed that capsaicin evoked a fast, transient depressor response that preceded the rise in BP (see arrow in Figs 9A and 10). At doses <4 μg/kg, bolus capsaicin only produced this transient depressor response accompanied by a decrease in heart rate of ~200 bpm ($P = 1.6 \times 10^{-6}$, Fig. 10A–C). At higher doses of capsaicin (>8 μg/kg), an additional pressor response emerged. Notably, pre-treatment with atropine or sensory nerve ablation eliminated this transient depressor response to capsaicin (Fig. 10A–C), consistent with its being mediated by the vagus nerve, and unmasked the arteriolar TRPV1-mediated increase in BP. Thus, TRPV1 in sensory nerves mediates the transient Bezold–Jarisch reflex while TRPV1 in arterioles mediates the increase in blood pressure.

Lysophosphatidic acid constricts arterioles and increases blood pressure via TRPV1

Next, we tested the potential physiological function of vascular TRPV1. We hypothesized that the vasoconstrictive effects of some endogenous bioactive lipids are mediated by TRPV1 activation. We examined lysophosphatidic acid (LPA), a vasoconstrictor lipid species generated by platelets and atherogenic plaques (Panchatcharam *et al.* 2008; Cui, 2011) that potentially activates TRPV1 (Nieto-Posadas *et al.* 2011). Notably, LPA species containing an unsaturated acyl chain are potent vasoconstrictors but whether cognate GPCRs for LPA ($LPA_{1–6}$) mediate these effects is uncertain (Panchatcharam *et al.* 2008; Kano *et al.* 2019). We found that LPA (C18:1) constricted (by ~70%, $P = 1.2 \times 10^{-6}$) skeletal muscle arterioles isolated from WT but not from TRPV1-null mice (Fig. 11A and B). Furthermore, systemic administration of LPA (60 μg/kg) triggered a Bezold–Jarisch reflex and an increase in BP (by ~30 mmHg, $P = 4.4 \times 10^{-6}$) in a TRPV1-dependent manner (Fig. 11C and D). Thus, TRPV1 mediates both the vasoconstrictive and BP effects of LPA. These data agree with previous observations that LPA exerts a pressor effect in several mammals (cats, rats and guinea pigs) but notably not in rabbits (Tokumura *et al.* 1978, 1985), which possess a hypofunctional TRPV1 channel (Gavva *et al.* 2004).

Vascular TRPV1 resists desensitization and mediates a persistent increase in blood pressure

In sensory nerves, TRPV1 ordinarily exhibits pronounced desensitization to agonists, reflected by a diminishing current response to repeated (tachyphylaxis) or sustained agonist application (Dray *et al.* 1989; Koplas *et al.* 1997). Indeed, in voltage-clamped sensory neurons we found that repeated application of capsaicin evoked progressively smaller inward currents (Fig. 12A–C); the mean initial current (1212 ± 1306 pA, $n = 4$) declined by ~80% with four applications of capsaicin. In contrast, in isolated arterial smooth muscle cells, capsaicin evoked non-declining currents; the mean initial current (135 ± 104 pA, $n = 5$) was maintained over four applications of capsaicin ($P = 7 \times 10^{-5}$). Furthermore, during sustained (90 s) capsaicin application, the evoked current markedly declined in sensory neurons and this effect was more pronounced under low cytoplasmic Ca^{2+} buffering conditions (~90% with 0.2 mM EGTA *versus* 60% with 5 mM EGTA, Fig. 12A, B and D), consistent with the

Ca^{2+} dependence of desensitization (Dray *et al.* 1989; Koplas *et al.* 1997). However, TRPV1 in ASM cells exhibited significantly less desensitization than in nodose neurons under these same Ca^{2+} buffering conditions (30%, $P = 0.0028$ and ~0%, $P = 7.19 \times 10^{-5}$ respectively). Thus, compared with sensory neurons TRPV1 in arteries is significantly more resistant to desensitization.

Similarly, repetitive or prolonged (5–20 min) systemic administration of capsaicin to mice evoked reproducible and sustained increases in BP (Fig. 12E–H). These pressor effects were unaffected by ablation of sensory nerves ($P = 0.99$, Fig. 12E and H) and occurred without changes in heart rate upon the elevated BP (Fig. 12F, G and J), reflecting a primary action of TRPV1 located in vascular myocytes. Finally, we tested whether LPA could generate persistent BP responses. Similar to capsaicin, slow infusion of LPA (C18:1, 75 μg/kg/min) produced sustained increases in BP without affecting heart rate (Fig. 12G, I and J).

Discussion

TRPV1 is an ion channel with important roles in somatosensory transduction (Caterina & Julius, 2001; Bautista *et al.* 2014). Our data reveal extensive expression of TRPV1 in the arterial circulation. Using combined molecular and functional analyses we found that TRPV1 localizes to the smooth muscle of arterioles supplying the skeletal muscle, heart and adipose tissues. Notably, we did not detect TRPV1 in vascular endothelium and removal of endothelium did not affect the efficacy/potency for capsaicin to constrict arteries. Our functional data agree with earlier findings that capsaicin elevates intracellular Ca^{2+} and/or constricts gracilis (Kark *et al.* 2008; Czikora *et al.* 2012, 2013) and cremaster (Cavanaugh *et al.* 2011) muscle arterioles. Here, we have extended these observations, revealing remarkable TRPV1 expression throughout the network of skeletal muscle arterioles (see Figs 3 and 6). Furthermore, we demonstrate for the first time TRPV1 expression and function in coronary, adipose and a subset of brain arterioles. Moreover, we show that TRPV1 predominates in small-diameter (<150 μm) arterioles and is practically absent in large vessels. Quantitative mRNA measurements showed that TRPV1 expression in small arterioles is ~13% of DRG levels. Similarly, the peak capsaicin-evoked current density in arterial smooth muscle cells was ~11% of that recorded in sensory neurons.

Several pertinent observations can be made about TRPV1 expression in vascular smooth muscle. First, given the extensive network of arteries in muscle and adipose tissues, the overall level of TRPV1 protein in the vasculature likely exceeds that in nerves. Second, activation of TRPV1, was capable of markedly constricting skeletal muscle arteries (both *ex vivo* and *in vivo*) and coronary arteries leading to reduced coronary perfusion. The L-type Ca^{2+} channel ($Ca_V1.2$) blocker nifedipine only partly inhibited the response to a saturating concentration of capsaicin, indicating that Ca^{2+} entry via maximally activated TRPV1 *per se* can support constriction while depolarization-induced activation of $Ca_V1.2$ amplifies the response. The amplification may become prominent during submaximal activation of TRPV1.

We found that systemic administration of TRPV1 agonists elicited large increases in BP. This pressor effect occurred without significant changes in heart rate and is consistent

with a vasoconstrictor action of TRPV1. Although TRPV1-expressing sensory nerves, through the release of vasoactive peptides, could contribute to changes in BP, we found the pressor response was independent of neurogenic regulation. First, we studied mice and rats treated after birth with RTX or capsaicin to ablate the TRPV1-positive sensory nerve population. TRPV1 in the vasculature of these animals exemplified complete recovery when measured at 8–10 weeks, reflecting lower toxicity and/or replacement by newly generated arterial smooth muscle cells. Notably, the BP response to capsaicin in these nerve-ablated animals was unchanged compared with control animals indicating that sensory nerves do not significantly contribute to TRPV1-mediated BP regulation. One exception to this result was the presence of a fast depressor response to capsaicin, most evident upon bolus administration. This BP decrease, accompanied by decreased heart rate and apnoea, likely reflects the Bezold–Jarisch reflex (Szolcsanyi *et al.* 1990) and was abolished after sensory nerve ablation or after atropine treatment to inhibit vagal cholinergic responses. Second, we found that TRPV1 channels in ASM cells are relatively resistant to capsaicin-induced desensitization. Significantly, this effect was recapitulated in systemic BP recordings where infusions of TRPV1 agonists produced sustained increases in BP without obvious desensitization. Furthermore, during repetitive capsaicin treatment we observed that the Bezold–Jarisch reflex was evident only upon the first administration consistent with a pronounced desensitization of sensory nerves. Taken together, the sustained increases in BP correlate with the persistent opening of TRPV1 channels in ASM cells and not with the transient TRPV1 response in sensory nerves. Our finding that sensory nerves play little role in the persistent capsaicin regulation of BP may seem surprising, but is consistent with many earlier studies showing that sensory nerves primarily trigger dilatation rather than constriction of arterioles, and that this effect is especially evident in the skin and other epithelial tissues (Baluk, 1997; Holzer, 1998). Similarly, capsaicin triggers marked plasma extravasation (measured by Evans Blue) that is restricted to the skin, airways and urogenital organs, which have prominent perivascular sensory nerves, and neurogenic inflammation is absent throughout the remainder of the circulation including brain, skeletal muscle and the heart (Saria *et al.* 1983; Baluk, 1997). Thus, any neurogenic vasodilatory action in response to systemic capsaicin would be swamped by the direct vasoconstrictor effects in arterioles.

What processes allow vascular smooth muscle TRPV1 to resist desensitization? The desensitization of TRPV1 is both Ca^{2+} and state dependent. In sensory nerves the removal of external Ca^{2+} ions abolishes capsaicin-induced desensitization consistent with a key role for Ca^{2+} signalling (Dray *et al.* 1989; Koplas *et al.* 1997). Direct binding of calmodulin (Numazaki *et al.* 2003), Ca^{2+}-induced dephosphorylation (Jung *et al.* 2004; Mohapatra & Nau, 2005) or Ca^{2+}-dependent hydrolysis of phosphatidylinositol 4,5-bisphosphate (Yao & Qin, 2009; Lukacs *et al.* 2013) have all been proposed as potential mechanisms. Further, structural changes in the TRPV1 channel may underlie desensitization. Evidence in support of this is provided by studies of the ultrapotent agonist RTX and double-knot spider toxin (DkTx), which do not induce desensitization even in the presence of external Ca^{2+}. The results of cryo-EM analysis (Cao *et al.* 2013) suggest that binding of RTX/DkTx stabilizes displacement of the pore helix, which is a mobile element in gating, to produce sustained channel opening. In contrast, capsaicin does not stabilize movement of the pore helix, but instead engages the lower channel gate (Cao *et al.* 2013) leading to

the appearance of flickery channel openings (Hui *et al.* 2003) which may facilitate the transition to desensitized states. Thus in arteries, the relative resistance to capsaicin-induced desensitization may arise from modifications to the TRPV1 channel protein (including reduced sensitivity to Ca^{2+} or less Ca^{2+} permeability), the existence of different Ca^{2+} signalling pathways, or simply as a consequence of lower channel density and reduced Ca^{2+} influx. Further studies are needed to understand the precise underlying mechanisms.

TRPV1 plays a critical role in pain signalling; diverse inflammatory mediators activate or sensitize TRPV1 located in sensory nerves to enhance nociception (Szallasi & Blumberg, 1999; Caterina & Julius, 2001; Basbaum *et al.* 2009). Our data reveal that TRPV1 agonists, including capsaicin and LPA, act on arterial TRPV1 to mediate vasoconstriction and a sustained increase in systemic BP. Notably, LPA is produced by platelets and artherogenic plaques (Panchatcharam *et al.* 2008; Cui, 2011) and is elevated in acute coronary syndrome (Dohi *et al.* 2012; Kurano *et al.* 2015) associated with vasospasm of small coronary arteries. TRPV1 in the coronary micro-circulation may therefore represent a prime target for mediating this vasoconstriction. Further, autotaxin, the rate-limiting enzyme for LPA production, is secreted abundantly by adipocytes (Dusaulcy *et al.* 2011) bringing the synthesis of LPA in close proximity to adipose arteries that highly express TRPV1. Notably, several lipoxygenase-dependent metabolites of arachidonic acid are potent TRPV1 agonists, including 12-(*S*)- and 15-(*S*)-hydroperoxyeicosatetraenoic acid, 5-(*S*)-, 5-(*R*)- and 12-(*S*)-hydroxyeicosatetraenoic acid, and leukotriene B_4 (Hwang *et al.* 2000) and may therefore be capable of constricting TRPV1-expressing arteries. Furthermore, capsaicin and related compounds commonly consumed in the diet could potentially affect arteries. However, whether dietary capsaicin can sufficiently raise plasma concentrations is unclear because of limited oral bioavailability (Rollyson *et al.* 2014). Genetic studies also support a role for TRPV1 in the regulation of blood flow. Indeed, disrupting TRPV1 gene expression exacerbates ischaemia–reperfusion injury in the heart (Wang & Wang, 2005). Furthermore, in experimentally induced sepsis, TRPV1-null mice exhibit both a greater fall in BP and higher mortality than their wild-type counter-parts (Clark *et al.* 2007; Wang *et al.* 2008; Guptill *et al.* 2011; Fernandes *et al.* 2012), suggesting that TRPV1-mediated vasoconstriction during inflammation contributes to the homeostatic regulation of BP. Collectively, these observations indicate potentially important roles for TRPV1 in regulating vasoconstriction and BP in disease and injury states. Finally, we point out that TRPV1 localizes to small arterioles that characteristically exhibit a high degree of spontaneous myogenic tone or vasomotion. Indeed, the pattern of TRPV1 expression in skeletal muscle arterioles that we report here matches the classical studies mapping myogenic tone in the limb and skeletal muscle arterial tree (Uchida & Bohr, 1969). These observations suggest potential regulatory roles for TRPV1 in vasomotor responses and we plan to address this hypothesis in future studies.

In summary, our data reveal extensive TRPV1 expression in arteriolar myocytes and show that activation of these TRPV1 channels profoundly affects regional/systemic vascular tone and blood pressure.

Acknowledgements

We thank Richard Gillis and Rosa Miyares for comments on the article.

Funding

This study was supported by National Institute of Diabetes and Digestive and Kidney Diseases Grant U01 DK-101040 (G.A.), the Hungarian Research Fund (OTKA K116940 to R.P. and A.T.) and by the GINOP-2.3.2-15-2016-00043 and GINOP-2.3.2-15-2016-00050 grants (to A.T.). The project is co-financed by the European Union and the European Regional Development Fund. H.G. was supported by Gedeon Richter Talentum Foundation (Budapest, Hungary).

Data availability statement

The data that support the findings of this study are available from the corresponding author upon reasonable request.

Supplementary Material

Refer to Web version on PubMed Central for supplementary material.

Biography

Thieu X. Phan received his PhD at the University of Bucharest in 2012. Since 2014 he has worked in the group of Dr Gerard Ahern at Georgetown University Medical Center in Washington, DC. He is interested in the functional properties of transient receptor potential (TRP) channels. Currently, he is focused on mapping the expression and function of TRPV1 in artery smooth muscle cells, and in particular, how TRPV1 regulates regional blood flow and blood pressure.

References

Baluk P (1997). Neurogenic inflammation in skin and airways. J Investig Dermatol Symp Proc 2, 76–81.

Basbaum AI, Bautista DM, Scherrer G & Julius D (2009). Cellular and molecular mechanisms of pain. Cell 139, 267–284. [PubMed: 19837031]

Bautista DM, Wilson SR & Hoon MA (2014). Why we scratch an itch: the molecules, cells and circuits of itch. Nat Neurosci 17, 175–182. [PubMed: 24473265]

Bohlen CJ, Priel A, Zhou S, King D, Siemens J & Julius D (2010). A bivalent tarantula toxin activates the capsaicin receptor, TRPV1, by targeting the outer pore domain. Cell 141, 834–845. [PubMed: 20510930]

Bratz IN, Dick GM, Tune JD, Edwards JM, Neeb ZP, Dincer UD & Sturek M (2008). Impaired capsaicin-induced relaxation of coronary arteries in a porcine model of the metabolic syndrome. Am J Physiol Heart Circ Physiol 294, H2489–H2496. [PubMed: 18390821]

Cao E, Liao M, Cheng Y & Julius D (2013). TRPV1 structures in distinct conformations reveal activation mechanisms. Nature 504, 113–118. [PubMed: 24305161]

Caterina MJ & Julius D (2001). The vanilloid receptor: a molecular gateway to the pain pathway. Annu Rev Neurosci 24, 487–517. [PubMed: 11283319]

Caterina MJ, Leffler A, Malmberg AB, Martin WJ, Trafton J, Petersen-Zeitz KR, Koltzenburg M, Basbaum AI & Julius D (2000). Impaired nociception and pain sensation in mice lacking the capsaicin receptor. Science 288, 306–313. [PubMed: 10764638]

Caterina MJ, Schumacher MA, Tominaga M, Rosen TA, Levine JD & Julius D (1997). The capsaicin receptor: a heat-activated ion channel in the pain pathway. Nature 389, 816–824. [PubMed: 9349813]

Cavanaugh DJ, Chesler AT, Jackson AC, Sigal YM, Yamanaka H, Grant R, O'Donnell D, Nicoll RA, Shah NM, Julius D & Basbaum AI (2011). Trpv1 reporter mice reveal highly restricted brain distribution and functional expression in arteriolar smooth muscle cells. J Neurosci 31, 5067–5077. [PubMed: 21451044]

Clark N, Keeble J, Fernandes ES, Starr A, Liang L, Sugden D, de Winter P & Brain SD (2007). The transient receptor potential vanilloid 1 (TRPV1) receptor protects against the onset of sepsis after endotoxin. FASEB J 21, 3747–3755. [PubMed: 17601984]

Cui M-Z (2011). Lysophosphatidic acid effects on atherosclerosis and thrombosis. Clin Lipidol 6, 413–426. [PubMed: 22162980]

Czikora Á, Lizanecz E, Bakó P, Rutkai I, Ruzsnavszky F, Magyar J, Pórszász R, Kark T, Facskó A, Papp Z, Edes I & Tóth A (2012). Structure-activity relationships of vanilloid receptor agonists for arteriolar TRPV1. Br J Pharmacol 165, 1801–1812. [PubMed: 21883148]

Czikora Á, Rutkai I, Pásztor ET, Szalai A, Pórszász R, Boczán J,Èdes I, Papp Z & Tóth A (2013). Different desensitization patterns for sensory and vascular TRPV1 populations in the rat: expression, localization and functional consequences. PLoS One 8, e78184. [PubMed: 24250792]

Davis JB, Gray J, Gunthorpe MJ, Hatcher JP, Davey PT, Overend P, Harries MH, Latcham J, Clapham C, Atkinson K, Hughes SA, Rance K, Grau E, Harper AJ, Pugh PL, Rogers DC, Bingham S, Randall A & Sheardown SA (2000). Vanilloid receptor-1 is essential for inflammatory thermal hyperalgesia. Nature 405, 183–187. [PubMed: 10821274]

Dohi T, Miyauchi K, Ohkawa R, Nakamura K, Kishimoto T, Miyazaki T, Nishino A, Nakajima N, Yaginuma K, Tamura H, Kojima T, Yokoyama K, Kurata T, Shimada K, Yatomi Y & Daida H (2012). Increased circulating plasma lysophosphatidic acid in patients with acute coronary syndrome. Clin Chim Acta 413, 207–212. [PubMed: 21983165]

Dray A, Bettaney J & Forster P (1989). Capsaicin desensitization of peripheral nociceptive fibres does not impair sensitivity to other noxious stimuli. Neurosci Lett 99, 50–54. [PubMed: 2748018]

Dusaulcy R, Rancoule C, Grès S, Wanecq E, Colom A, Guigné C, Van Meeteren LA, Moolenaar WH, Valet P & Saulnier-Blache JS (2011). Adipose-specific disruption of autotaxin enhances nutritional fattening and reduces plasma lysophosphatidic acid. J Lipid Res 52, 1247–1255. [PubMed: 21421848]

Fernandes ES, Liang L, Smillie S-J, Kaiser F, Purcell R, Rivett DW, Alam S, Howat S, Collins H, Thompson SJ, Keeble JE, Riffo-Vasquez Y, Bruce KD & Brain SD (2012). TRPV1 deletion enhances local inflammation and accelerates the onset of systemic inflammatory response syndrome. J Immunol 188, 5741–5751. [PubMed: 22547700]

Fischer MJM, Uchida S & Messlinger K (2010). Measurement of meningeal blood vessel diameter in vivo with a plug-in for Image. J Microvasc Res 80, 258–266.

Gao Y, Cao E, Julius D & Cheng Y (2016). TRPV1 structures in nanodiscs reveal mechanisms of ligand and lipid action. Nature 534, 347–351. [PubMed: 27281200]

Gavva NR, Klionsky L, Qu Y, Shi L, Tamir R, Edenson S, Zhang TJ, Viswanadhan VN, Toth A, Pearce LV, Vanderah TW, Porreca F, Blumberg PM, Lile J, Sun Y, Wild K, Louis J-C & Treanor JJS (2004). Molecular determinants of vanilloid sensitivity in TRPV1. J Biol Chem 279, 20283–20295. [PubMed: 14996838]

Guptill V, Cui X, Khaibullina A, Keller JM, Spornick N, Mannes A, Iadarola M & Quezado ZMN (2011). Disruption of the transient receptor potential vanilloid 1 can affect survival, bacterial clearance, and cytokine gene expression during murine sepsis. Anesthesiology 114, 1190–1199. [PubMed: 21383614]

Holzer P (1998). Neurogenic vasodilatation and plasma leakage in the skin. Gen Pharmacol 30, 5–11. [PubMed: 9457475]

Hui K, Liu B & Qin F (2003). Capsaicin activation of the pain receptor, VR1: multiple open states from both partial and full binding. Biophys J 84, 2957–2968. [PubMed: 12719227]

Hwang SW, Cho H, Kwak J, Lee SY, Kang CJ, Jung J, Cho S, Min KH, Suh YG, Kim D & Oh U (2000). Direct activation of capsaicin receptors by products of lipoxygenases: Endogenous capsaicin-like substances. Proc Natl Acad Sci U S A 97, 6155–6160. [PubMed: 10823958]

Jancsó G, Kiraly E & Jancsó-Gábor A (1977). Pharmacologically induced selective degeneration of chemosensitive primary sensory neurones. Nature 270, 741–743. [PubMed: 593396]

Jancsó G & Sántha P (2015). The foundation of sensory pharmacology: Nicholas (Miklós) Jancsó and the Szeged contribution. Temperature 2, 152–157.

Jung J, Shin JS, Lee S-Y, Hwang SW, Koo J, Cho H & Oh U (2004). Phosphorylation of vanilloid receptor 1 by Ca^{2+}/calmodulin-dependent kinase II regulates its vanilloid binding. J Biol Chem 279, 7048–7054. [PubMed: 14630912]

Kano K, Matsumoto H, Inoue A, Yukiura H, Kanai M, Chun J, Ishii S, Shimizu T & Aoki J (2019). Molecular mechanism of lysophosphatidic acid-induced hypertensive response. Sci Rep 9, 2662. [PubMed: 30804442]

Kark T, Bagi Z, Lizanecz E, Pásztor ET, Erdei N, Czikora A, Papp Z, Edes I, Pórszász R & Tóth A (2008). Tissue-specific regulation of microvascular diameter: opposite functional roles of neuronal and smooth muscle located vanilloid receptor-1. Mol Pharmacol 73, 1405–1412. [PubMed: 18256211]

Koplas PA, Rosenberg RL & Oxford GS (1997). The role of calcium in the desensitization of capsaicin responses in rat dorsal root ganglion neurons. J Neurosci 17, 3525–3537. [PubMed: 9133377]

Kurano M, Suzuki A, Inoue A, Tokuhara Y, Kano K, Matsumoto H, Igarashi K, Ohkawa R, Nakamura K, Dohi T, Miyauchi K, Daida H, Tsukamoto K, Ikeda H, Aoki J & Yatomi Y (2015). Possible involvement of minor lysophospholipids in the increase in plasma lysophosphatidic acid in acute coronary syndrome. Arterioscler Thromb Vasc Biol 35, 463–470. [PubMed: 25425621]

Liao M, Cao E, Julius D & Cheng Y (2013). Structure of the TRPV1 ion channel determined by electron cryo-microscopy. Nature 504, 107–112. [PubMed: 24305160]

Lizanecz E, Bagi Z, Pásztor ET, Papp Z, Edes I, Kedei N, Blumberg PM & Tóth A (2006). Phosphorylation-dependent desensitization by anandamide of vanilloid receptor-1 (TRPV1) function in rat skeletal muscle arterioles and in Chinese hamster ovary cells expressing TRPV1. Mol Pharmacol 69, 1015–1023. [PubMed: 16338989]

Lukacs V, Yudin Y, Hammond GR, Sharma E, Fukami K & Rohacs T (2013). Distinctive changes in plasma membrane phosphoinositides underlie differential regulation of TRPV1 in nociceptive neurons. J Neurosci 33, 11451–11463. [PubMed: 23843517]

Mishra SK, Tisel SM, Orestes P, Bhangoo SK & Hoon MA (2011). TRPV1-lineage neurons are required for thermal sensation. EMBO J 30, 582–593. [PubMed: 21139565]

Mohapatra DP & Nau C (2005). Regulation of Ca^{2+}-dependent desensitization in the vanilloid receptor TRPV1 by calcineurin and cAMP-dependent protein kinase. J Biol Chem 280, 13424–13432. [PubMed: 15691846]

Nieto-Posadas A, Picazo-Juárez G, Llorente I, Jara-Oseguera A, Morales-Lázaro S, Escalante-Alcalde D, Islas LD & Rosenbaum T (2011). Lysophosphatidic acid directly activates TRPV1 through a C-terminal binding site. Nat Chem Biol 8, 78–85. [PubMed: 22101604]

Numazaki M, Tominaga T, Takeuchi K, Murayama N, Toyooka H & Tominaga M (2003). Structural determinant of TRPV1 desensitization interacts with calmodulin. Proc Natl Acad Sci U S A 100, 8002–8006. [PubMed: 12808128]

Panchatcharam M, Miriyala S, Yang F, Rojas M, End C, Vallant C, Dong A, Lynch K, Chun J, Morris AJ & Smyth SS (2008). Lysophosphatidic acid receptors 1 and 2 play roles in regulation of vascular injury responses but not blood pressure. Circ Res 103, 662–670. [PubMed: 18703779]

Phan TX, Ton HT, Chen Y, Basha ME & Ahern GP (2016). Sex-dependent expression of TRPV1 in bladder arterioles. Am J Physiol Renal Physiol, 311, F1063–F1073. [PubMed: 27654891]

Rollyson WD, Stover CA, Brown KC, Perry HE, Stevenson CD, McNees CA, Ball JG, Valentovic MA & Dasgupta P (2014). Bioavailability of capsaicin and its implications for drug delivery. J Control Release 196, 96–105. [PubMed: 25307998]

Sand CA, Grant AD & Nandi M (2015). Vascular expression of transient receptor potential vanilloid 1 (TRPV1). J Histochem Cytochem 63, 449–453. [PubMed: 25809792]

Saria A, Lundberg JM, Skofitsch G & Lembeck F (1983). Vascular protein linkage in various tissue induced by substance P, capsaicin, bradykinin, serotonin, histamine and by antigen challenge. Naunyn Schmiedebergs Arch Pharmacol 324, 212–218. [PubMed: 6197659]

Szallasi A & Blumberg PM (1992). Vanilloid receptor loss in rat sensory ganglia associated with long term desensitization to resiniferatoxin. Neurosci Lett 140, 51–54. [PubMed: 1407700]

Szallasi A & Blumberg PM (1999). Vanilloid (Capsaicin) receptors and mechanisms. Pharmacol Rev 51, 159–212. [PubMed: 10353985]

Szallasi A, Cortright DN, Blum CA & Eid SR (2007). The vanilloid receptor TRPV1: 10 years from channel cloning to antagonist proof-of-concept. Nat Rev Drug Discov 6, 357–372. [PubMed: 17464295]

Szolcsanyi J, Szallasi A, Szallasi Z, Joo F & Blumberg PM (1990). Resiniferatoxin: an ultrapotent selective modulator of capsaicin-sensitive primary afferent neurons. J Pharmacol Exp Ther 255, 923–928. [PubMed: 2243359]

Tokumura A, Fukuzawa K & Tsukatani H (1978). Effects of synthetic and natural lysophosphatidic acids on the arterial blood pressure of different animal species. Lipids 13, 572–574. [PubMed: 703535]

Tokumura A, Maruyama T, Fukuzawa K & Tsukatani H (1985). Effects of lysophosphatidic acids and their structural analogs on arterial blood pressure of cats. Arzneim-Forsch 35, 287–292. [PubMed: 3846454]

Tominaga M, Caterina MJ, Malmberg AB, Rosen TA, Gilbert H, Skinner K, Raumann BE, Basbaum AI & Julius D (1998). The cloned capsaicin receptor integrates multiple pain-producing stimuli. Neuron 21, 531–543. [PubMed: 9768840]

Toth A, Czikora A, Pasztor ET, Dienes B, Bai P, Csernoch L, Rutkai I, Csato V, Manyine IS, Porszasz R, Edes I, Papp Z & Boczan J (2014). Vanilloid receptor-1 (TRPV1) expression and function in the vasculature of the rat. J Histochem Cytochem 62, 129–144. [PubMed: 24217926]

Uchida E & Bohr DF (1969). Myogenic tone in isolated perfused vessels. Occurrence among vascular beds and along vascular trees. Circ Res 25, 549–555. [PubMed: 4981854]

Wang L & Wang DH (2005). TRPV1 gene knockout impairs postischemic recovery in isolated perfused heart in mice. Circulation 112, 3617–3623. [PubMed: 16314376]

Wang Y, Novotny M, Quaiserová-Mocko V, Swain GM & Wang DH (2008). TRPV1-mediated protection against endotoxin-induced hypotension and mortality in rats. Am J Physiol Regul Integr Comp Physiol 294, R1517–R1523. [PubMed: 18337316]

Yang D, Luo Z, Ma S, Wong WT, Ma L, Zhong J, He H, Zhao Z, Cao T, Yan Z, Liu D, Arendshorst WJ, Huang Y, Tepel M & Zhu Z (2010). Activation of TRPV1 by dietary capsaicin improves endothelium-dependent vasorelaxation and prevents hypertension. Cell Metab 12, 130–141. [PubMed: 20674858]

Yao J & Qin F (2009). Interaction with phosphoinositides confers adaptation onto the TRPV1 pain receptor. PLoS Biol 7, e1000046.

Yarmolinsky DA, Peng Y, Pogorzala LA, Rutlin M, Hoon MA & Zuker CS (2016). Coding and plasticity in the mammalian thermosensory system. Neuron 92, 1079–1092. [PubMed: 27840000]

Zygmunt PM, Petersson J, Andersson DA, Chuang H, Sorgard M, Di Marzo V, Julius D & Hogestatt ED (1999). Vanilloid receptors on sensory nerves mediate the vasodilator action of anandamide. Nature 400, 452–457. [PubMed: 10440374]

Key points

- The functional roles of the capsaicin receptor, TRPV1, outside of sensory nerves are unclear. We mapped TRPV1 in the mouse circulation, revealing extensive expression in the smooth muscle of resistance arterioles supplying skeletal muscle, heart and adipose tissue.
- Activation of TRPV1 in vascular myocytes constricted arteries, reduced coronary flow in isolated hearts and increased systemic blood pressure. These functional effects were retained after sensory nerve ablation, indicating specific signalling by arterial TRPV1.
- TRPV1 mediated the vasoconstrictive and blood pressure responses to the endogenous inflammatory lipid lysophosphatidic acid.
- These results show that TRPV1 in arteriolar myocytes modulates regional blood flow and systemic blood pressure, and suggest that TRPV1 may be a target of vasoactive inflammatory mediators.

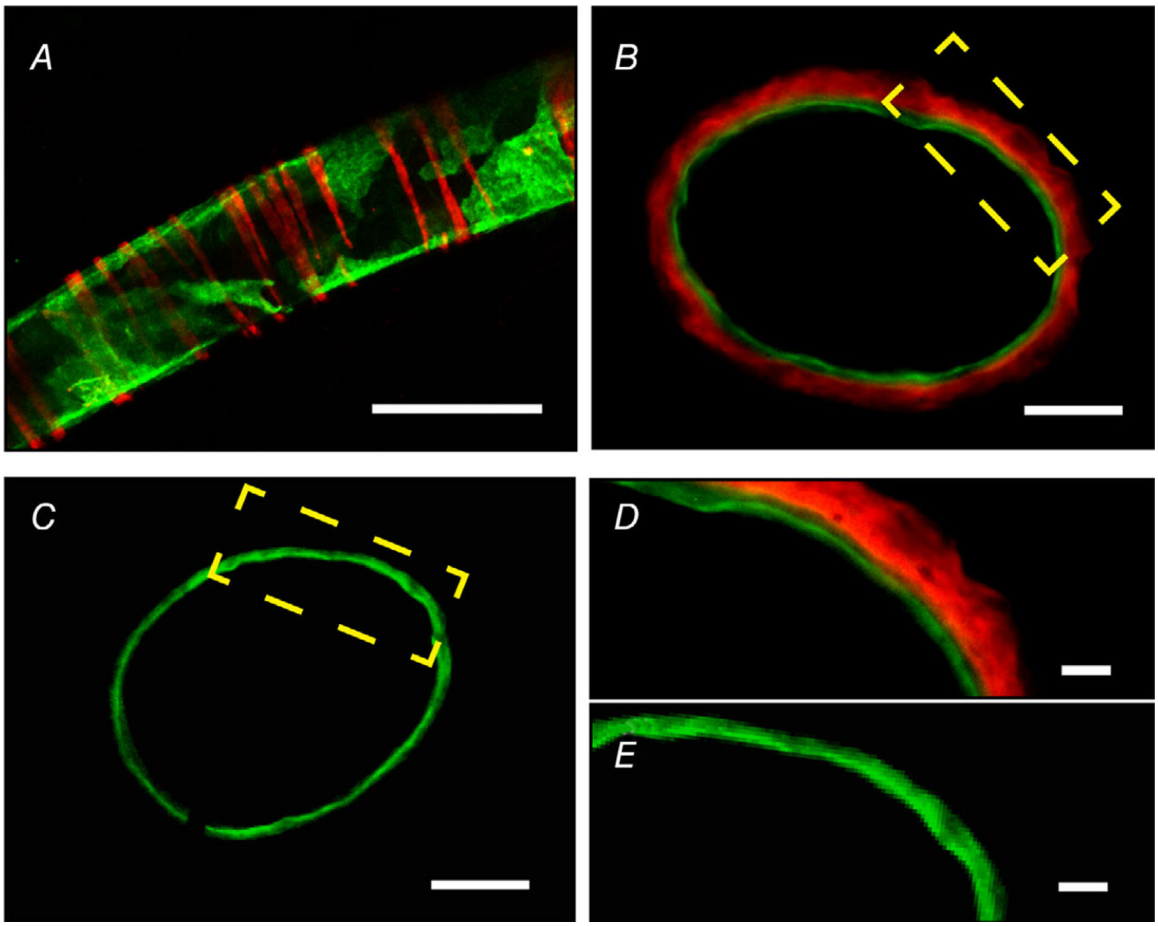

Figure 1. TRPV1 expression in arteries is restricted to vascular smooth muscle

A, TdTomato fluorescence in a muscle artery from a TRPV1-Cre:Tomato mouse. The endothelium is stained with DioC18 (green). Data were obtained from >4 arteries from 5 mice. *B*–*E*, LacZ and CD31 immunostaining in artery cross-sections from a $TRPV1^{PLAP\text{-}nlacZ}$ (*B* and *D*) and WT (*C* and *E*) mouse. Scale bar: 100 μm (*A*), 20 μm (*B* and *C*), 10 μm (*D* and *E*). Data were obtained from >3 arterial sections from 3 mice.

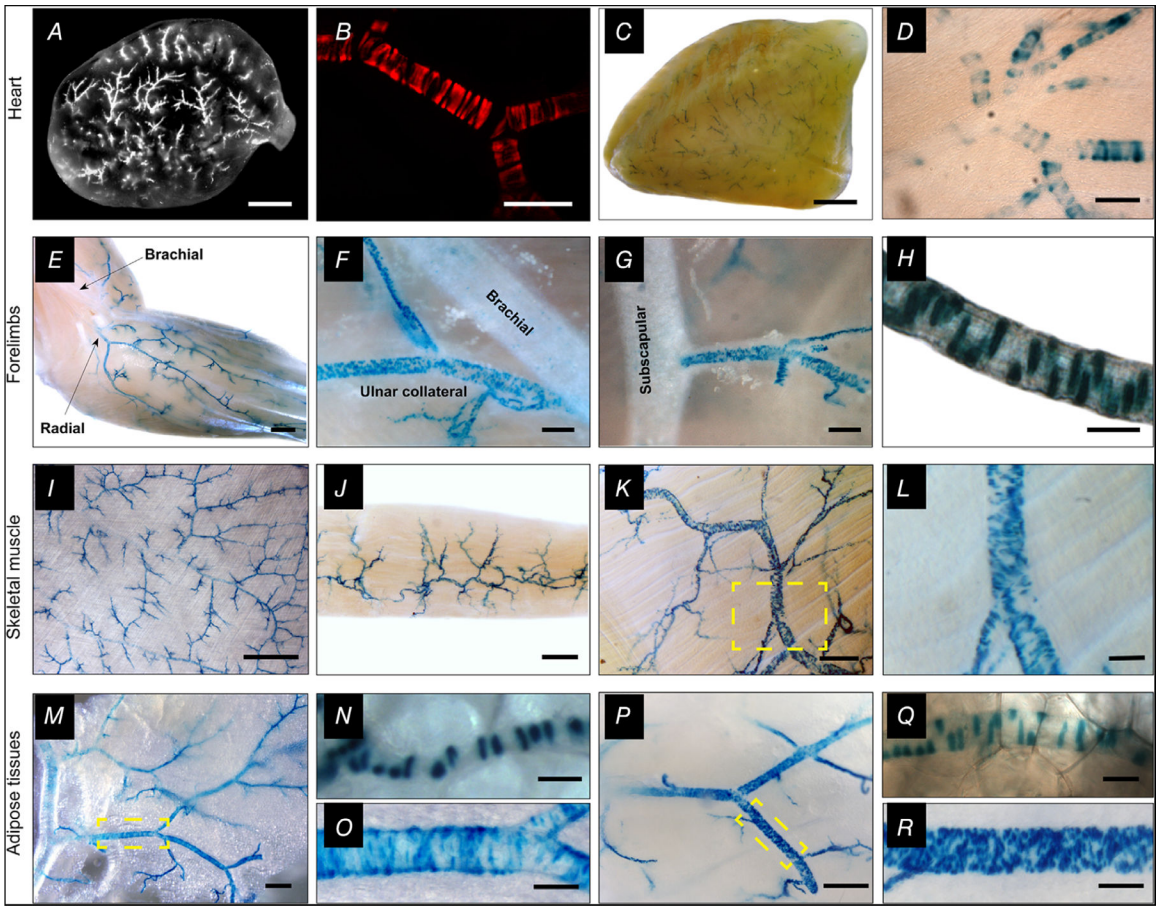

Figure 2. TRPV1 expression in arteriolar smooth muscle of the myocardium, skeletal muscle and adipose

A–D, analysis of whole hearts and transverse heart sections from TRPV1-Cre:tdTomato or TRPV1$^{PLAP\text{-}nlacZ}$ mice reveals TRPV1 expression in small arterioles of the ventricular myocardium. *E–R*, nuclear LacZ staining in forelimb arteries (*E–H*), arteries in latissimus dorsi, gracilis and trapezius skeletal muscles (*I–L*), and arteries supplying white (*M–O*) and brown (*P–R*) adipose tissues. Insets (yellow boxes) in *K*, *M* and *P* are expanded in *L*, *O* and *R*, respectively. Scale bar: 1 mm (*A*, *C*, *E*, *I*), 300 μm (*F*, *J*, *M*, *P*), 100 μm (*B*, *D*, *G*, *L*, *O*, *R*), 20 μm (*H*, *N*, Q). These representative images were compiled from a total of 30 male mice and six female mice and no apparent sex differences were noted.

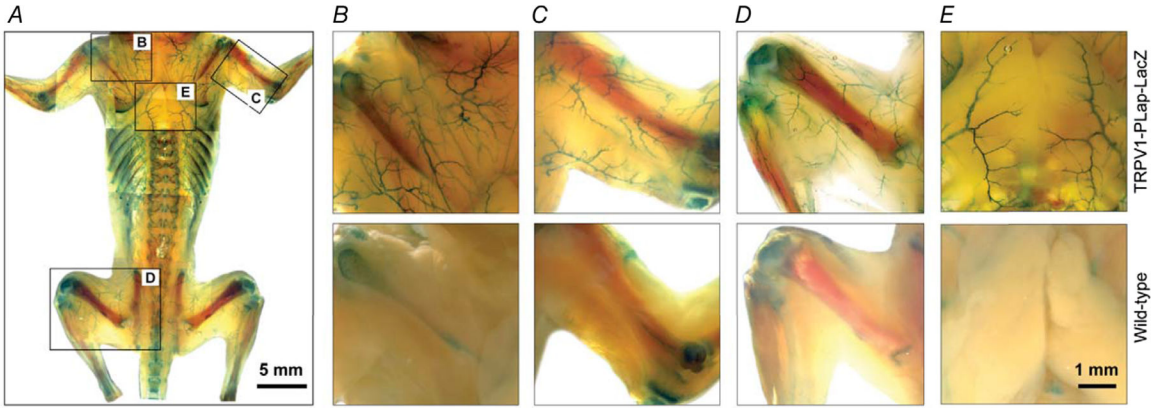

Figure 3. Arterial TRPV1 expression in a whole mouse preparation

Representative whole-animal nLacZ staining in a 2-week-old TRPV1$^{PLAP\text{-}nlacZ}$ mouse (skin removed) *versus* a control (wild-type) mouse shows extensive arterial TRPV1 expression in skeletal muscles (*A*–*D*) and interscapular brown adipose tissue (*E*). Note the non-specific staining in bone tissues. Data are representative of five TRPV1$^{PLAP\text{-}nlacZ}$ and two wild-type mice.

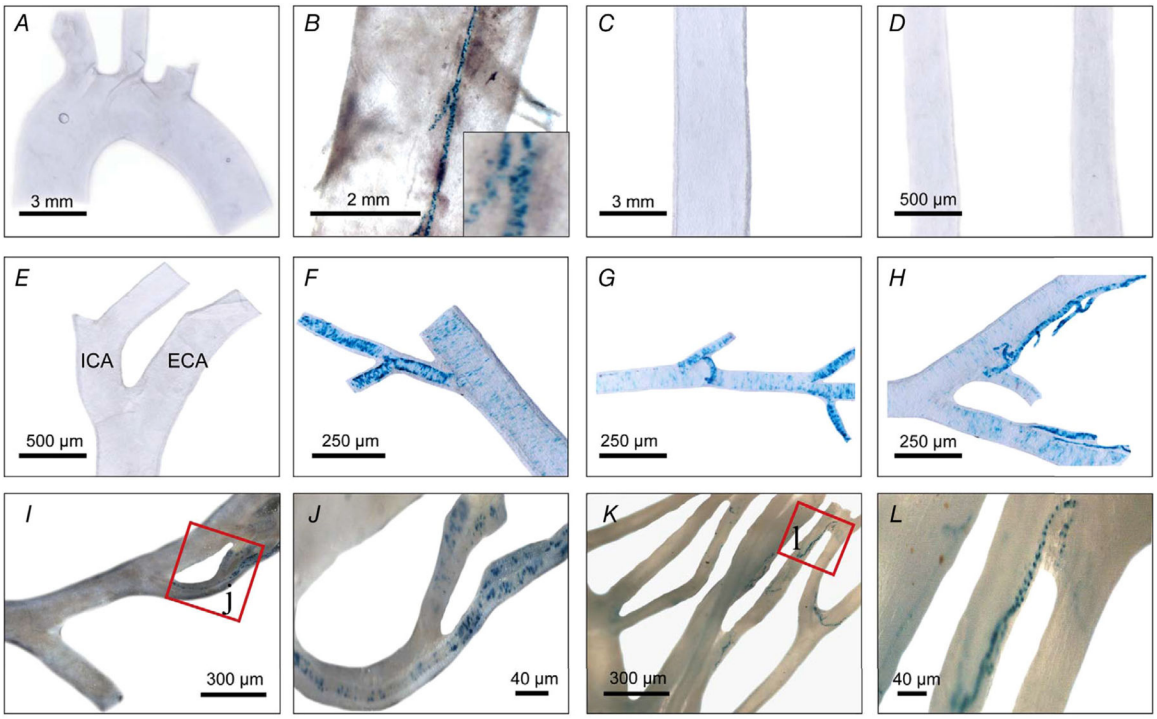

Figure 4. Limited TRPV1 expression in major mouse arteries

A and *B*, nLacZ staining in the aortic arch (*A*) and descending aorta (*B*) showing TRPV1 expression is restricted to small feeding arteries 'vasa vasorum' (see inset). *C–L*, abdominal aorta (*C*), common carotid (*D*) and external (ECA) and internal carotid (ICA) arteries (*E*), facial artery (*F*), maxillary artery (*G*), superficial temporal artery (*H*) and mesenteric arteries (*I–L*) (note restricted expression to small diameter branches). Data were compiled from 10 mice.

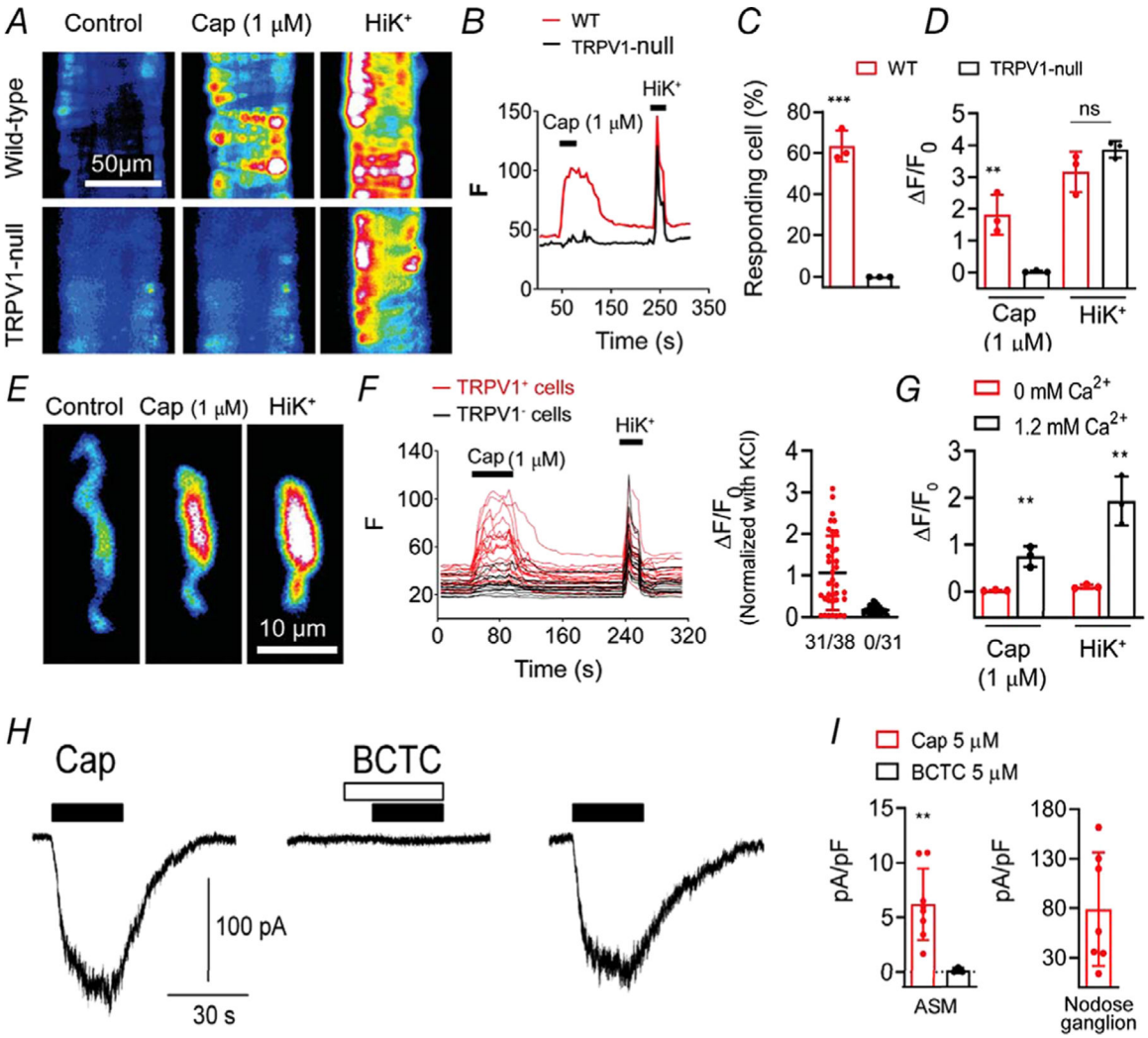

Figure 5. TRPV1 functionality in arterial smooth muscle cells

A–D, Ca^{2+} transients evoked by capsaicin (1 μM) and KCl (50 mM) in isolated cerebellar arteries from wild-type and TRPV1-null mice (n = 40–70 cells in the groups from three independent experiments, unpaired t test, ***P < 0.001; **P = 0.0079 and ns, P = 0.15). *E* and *F*, Capsaicin-evoked Ca^{2+} signalling in dissociated ASM cells from TRPV1-Cre:tdTomato mice is restricted to $TRPV1^{+}$ cells (31/38 $TRPV1^{+}$ and 0/31 $TRPV1^{-/-}$ cells). *G*, capsaicin- and K^{+}-evoked responses require extracellular Ca^{2+} (0 mM Ca^{2+}, n = 20, 1.2 mM Ca^{2+}, n = 30; unpaired t test, **P < 0.01. *H*, representative current traces in a voltage-clamped (−50 mV) ASM cell (10 pF) in response to capsaicin (filled bars, 5 μM) with or without the TRPV1 antagonist BCTC (open bars, 5 μM), and recovery after washout. *I*, mean current density in ASM cells in response to capsaicin (n = 9) and capsaicin + BCTC (n = 3, unpaired t test, **P = 0.0013) and in nodose ganglion neurons (n = 7).

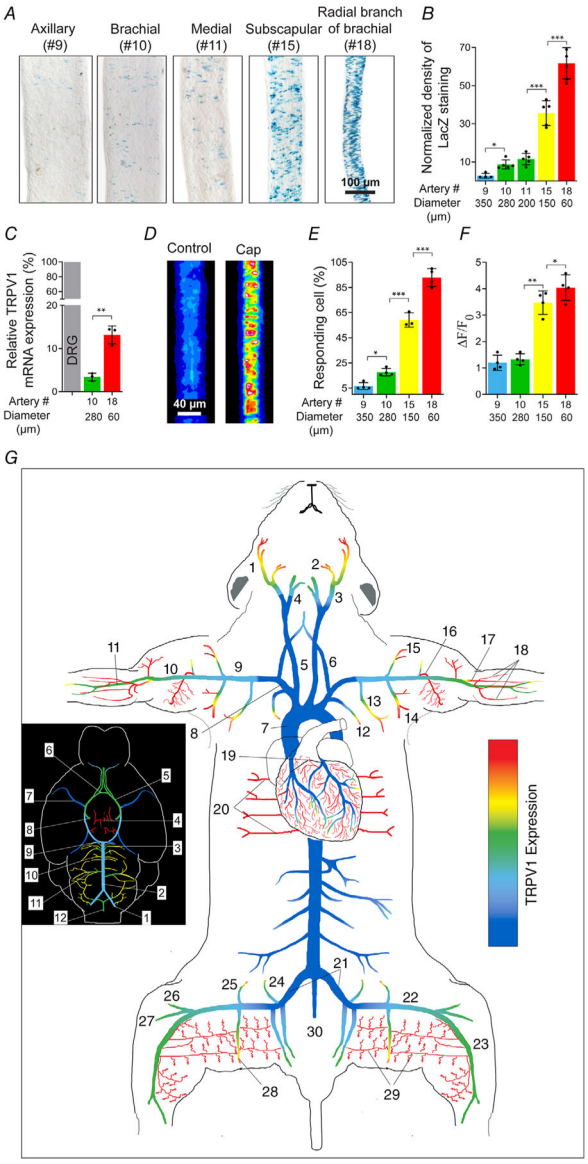

Figure 6. An arterial map of functional TRPV1 expression

A and *B*, TRPV1 expression (nuclear LacZ staining) in forelimb arteries and muscle branches *versus* vessel diameter ($n = 4$–6 arteries from five mice per group, one-way ANOVA, $^{*}P < 0.05$, $^{***}P < 0.001$). *C*, TRPV1 mRNA measured by qRT-PCR in small and large-diameter arteries relative to DRG ($n = 3$–4 mice, unpaired *t* test, $^{**}P = 0.0017$. *D*–*F*, capsaicin (1 μM)-evoked Ca^{2+} responses in forelimb arteries of different diameter (no. 9, $n = 85$; no. 10, $n = 92$; no. 15, $n = 136$; no. 18, $n = 150$ from three independent experiments, one-way ANOVA, $^{*}P < 0.05$, $^{**}P = 0.0029$, $^{***}P < 0.001$). *G*, heat-map of TRPV1 expression in arteries based on $TRPV1^{PLAP\text{-}nlacZ}$ mice ($n = 15$ mice) and confirmed by functional imaging. The inset shows the density of TRPV1 expression in cerebral arteries. Arterial colour-coding is similarly applied to *B*–*F*. Artery nomenclature is included in Table 1.

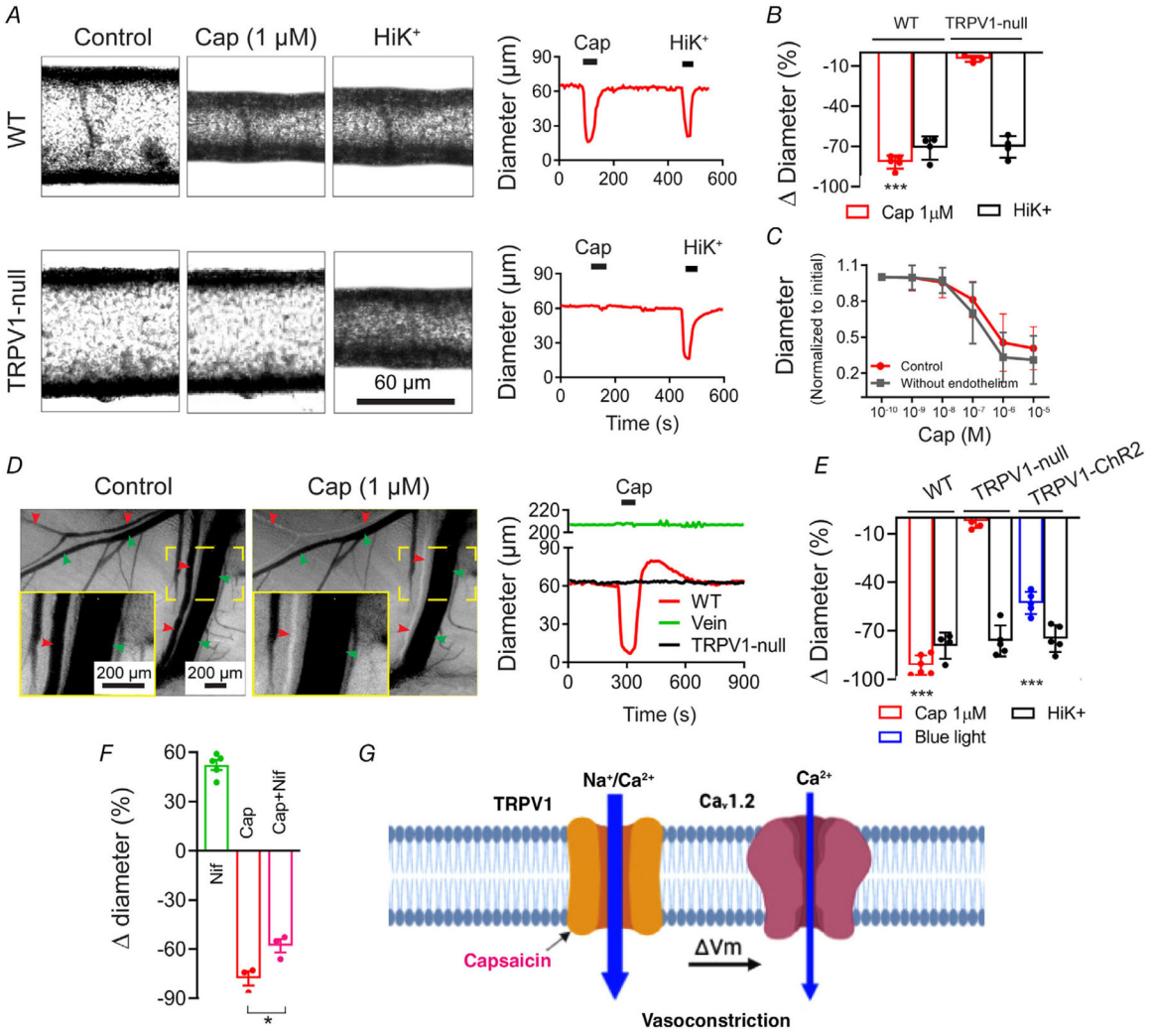

Figure 7. TRPV1 agonists constrict skeletal muscle arterioles

A and *B*, capsaicin (1 μM) constricts isolated, pressurized (60 mmHg) skeletal muscle arteries from wild-type but not TRPV1-null mice (WT, $n = 5$; TRPV1-null, $n = 4$; unpaired *t* test, $^{***}P < 0.001$). *C*, capsaicin constricts intact and endothelium-denuded gracilis arteries from rats with similar potency ($n = 6$). *D* and *E*, intravital imaging shows that capsaicin constricts radial branch arteries (red arrowheads) without affecting veins (green arrowheads). The insets (continuous yellow boxes) show expanded views of the designated area (dashed yellow boxes). Arteries from TRPV1-null mice are unresponsive to capsaicin and blue-light constricts arteries from TRPV1-Cre:ChR2 mice (WT, $n = 7$; KO, $n = 5$; TRPV1-ChR2, $n = 5$ arteries obtained from 3 (KO and TRPV1-ChR2) and 5 (WT) mice, one-way ANOVA, $^{***}P < 0.001$). *F*, *in vivo* arteriole diameter following treatment with nifidepine (3 μM, $n = 5$), capsaicin (1 μM, $n = 3$), and nifedipine–capsaicin ($n = 3$, from three mice, unpaired *t* test, $^{*}P = 0.027$). *G*, proposed model for Ca^{2+}-entry pathways underlying capsaicin-induced vasoconstriction.

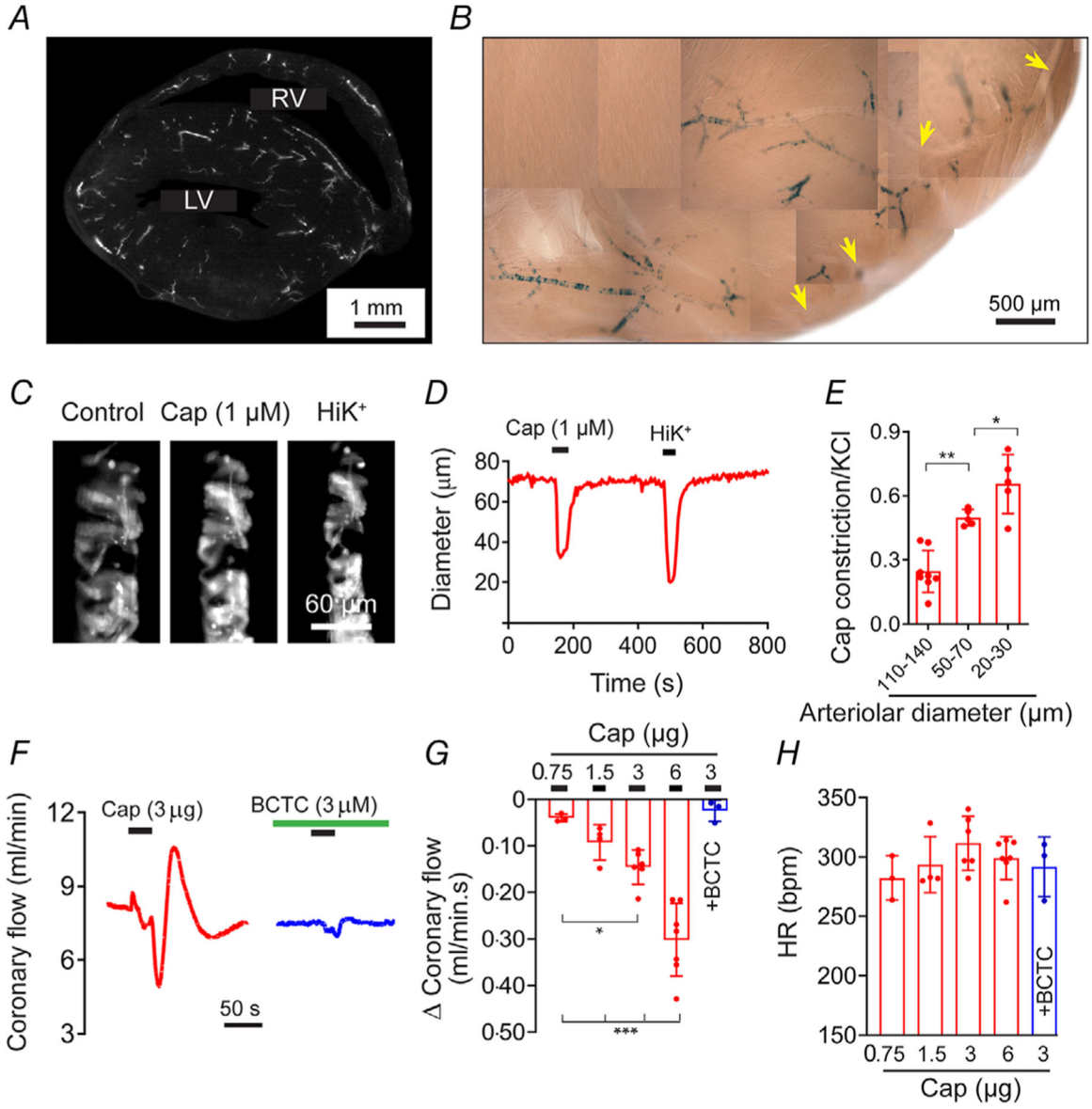

Figure 8. Capsaicin constricts coronary arterioles and reduces coronary perfusion

A and *B*, sagittal sections (150 µm) of hearts from TRPV1-Cre:tdTomato and TRPV1-nLacZ mice reveal TRPV1 expression in small arteriole branches (yellow arrowheads denote the left coronary artery). *C–E*, capsaicin preferentially constricts small arterioles *in situ* in slice preparations from the hearts of TRPV1-Cre:tdTomato mice. Data are normalized to KCl (40 mM) ($n = 5$, one-way ANOVA, $^{*}P < 0.05$, $^{**}P < 0.01$). *F–H*, capsaicin dose-dependently decreases coronary perfusion in isolated rat hearts ($n = 7$) without affecting the heart rate. BCTC ($n = 3$) abolishes the effect of capsaicin (one-way ANOVA, $^{*}P < 0.05$, $^{***}P < 0.001$).

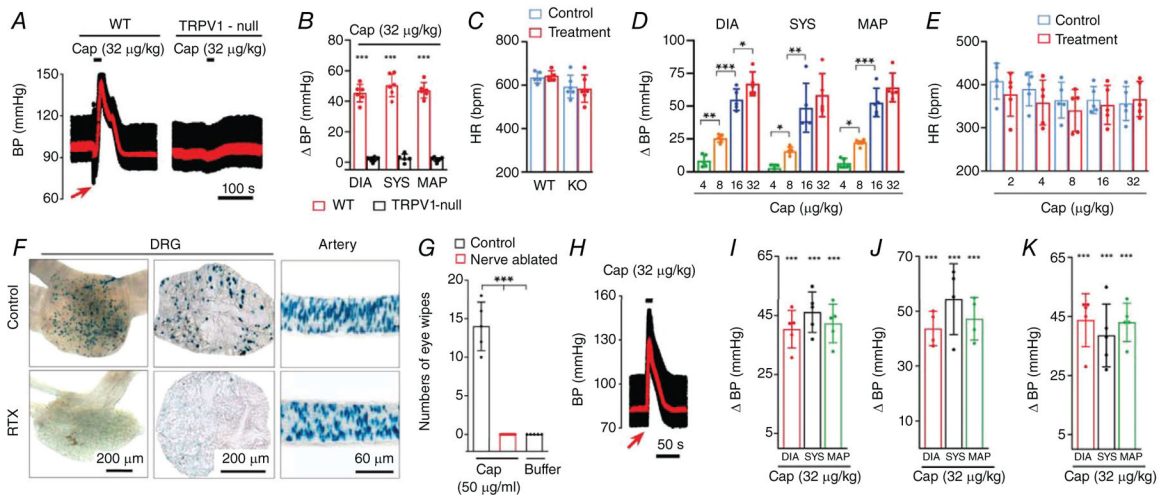

Figure 9. Arterial TRPV1 regulates systemic blood pressure

A–C, blood pressure (BP) and heart rate (HR) changes in wild-type and TRPV1-null mice in response to intravenous (I.V.) infusion (20 s) of capsaicin ($n = 4–7$, unpaired t test, $^{***}P < 0.001$). Mean arterial pressure (MAP) is shown in red. *D* and *E*, mean changes in systolic BP, diastolic BP, MAP and HR in rats during bolus I.V. capsaicin ($n = 6$, one-way ANOVA, $^{*}P = 0.0475$, $^{**}P < 0.01$, $^{***}P < 0.001$). *F*, nuclear LacZ staining in L5 dorsal root ganglion (section and whole ganglion) and arteries from mice with or without neonatal RTX treatment. *G*, mean eye-wipes in response to buffer ($n = 5$), or capsaicin in control ($n = 5$) and nerve-ablated rats ($n = 14$, one-way ANOVA, $^{***}P < 0.001$). *H* and *I*, BP responses to I.V. capsaicin in sensory nerve ablated mice ($n = 5$, unpaired t test, $^{***}P < 0.001$) and *J*, rats ($n = 4$, unpaired t test, $^{***}P < 0.001$). *K*, change in BP in conscious mice (nerve ablated) in response to I.V. administration (20 s) of capsaicin ($n = 5$, unpaired t test, $^{***}P < 0.001$).

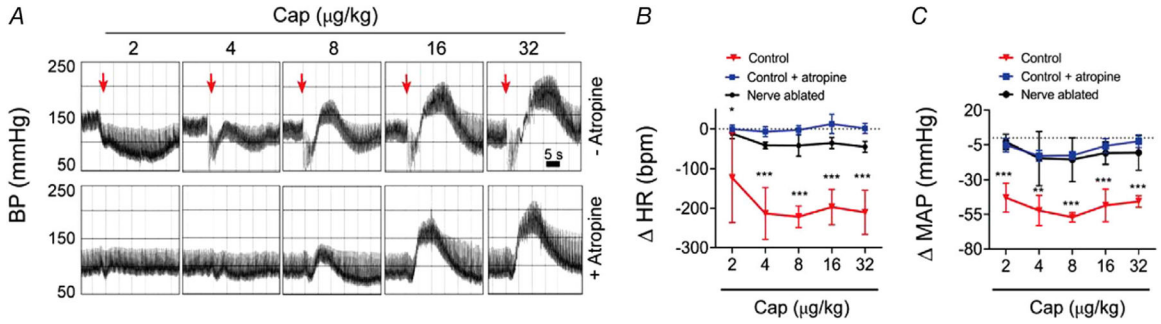

Figure 10. TRPV1 in sensory nerves mediates the Bezold-Jarisch reflex

A, BP recordings in a rat in response to escalating bolus I.V. doses of capsaicin with or without atropine pre-treatment (note: atropine abolishes the rapid decrease in BP reflecting a Bezold–Jarisch reflex). *B* and *C*, mean changes in HR and MAP measured immediately after bolus I.V. capsaicin in control, atropine-treated or sensory nerve ablated rats ($n = 6$, one-way ANOVA, $*P < 0.05$, $**P < 0.01$, $***P < 0.001$).

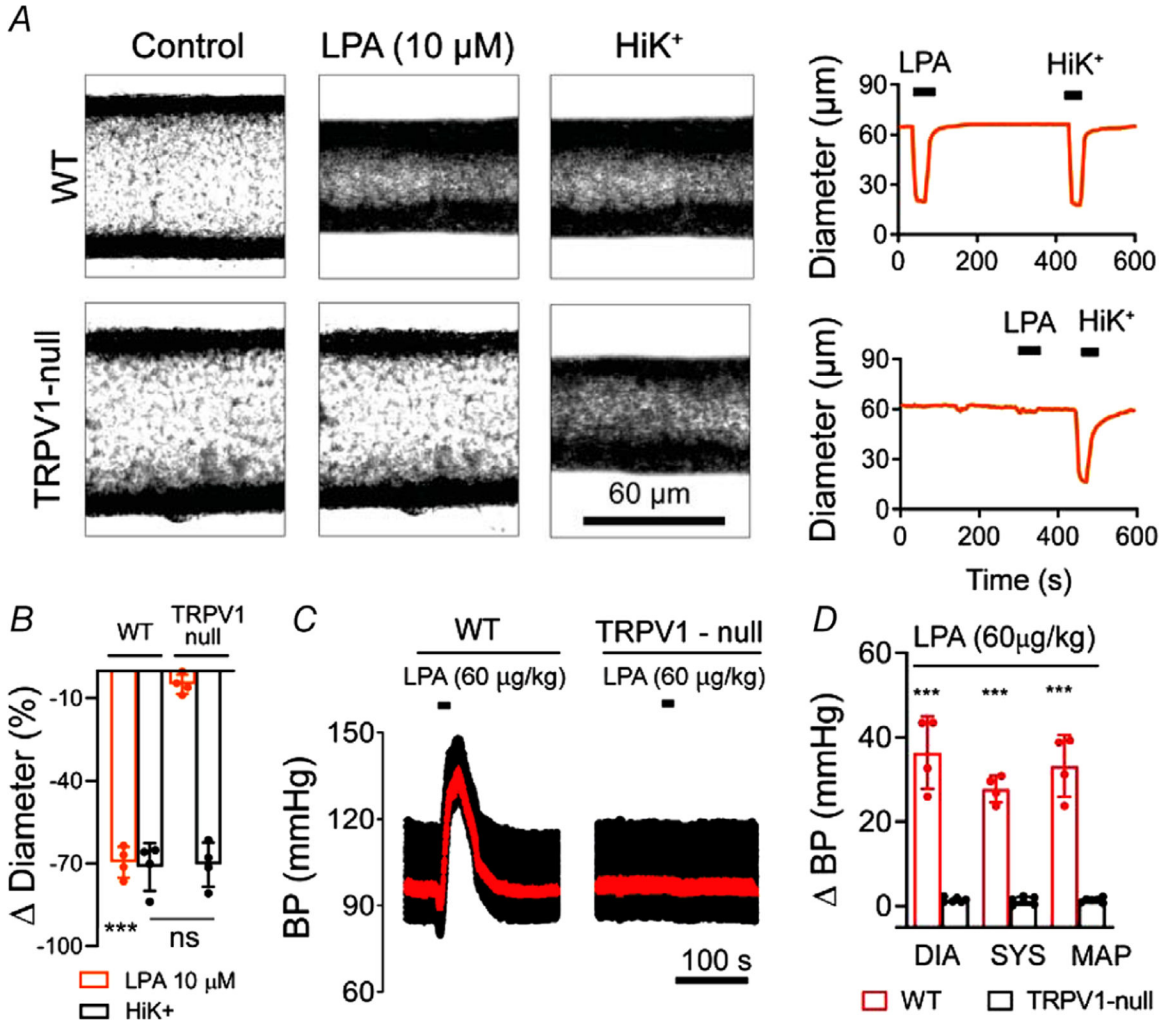

Figure 11. TRPV1 is critical for lysophosphatidic acid-induced vasoconstriction

A and *B*, LPA (C18:1, 10 μM) constricts isolated, pressurized (60 mmHg) skeletal muscle arteries from wild-type but not TRPV1-null mice ($n = 4$, unpaired t test, $^{***}P < 0.001$). *C* and *D*, BP changes in wild-type ($n = 4$) and TRPV1-null ($n = 6$) mice in response to I.V. infusion (20 s)=of LPA (C18:1; unpaired t test, $^{***}P < 0.001$).

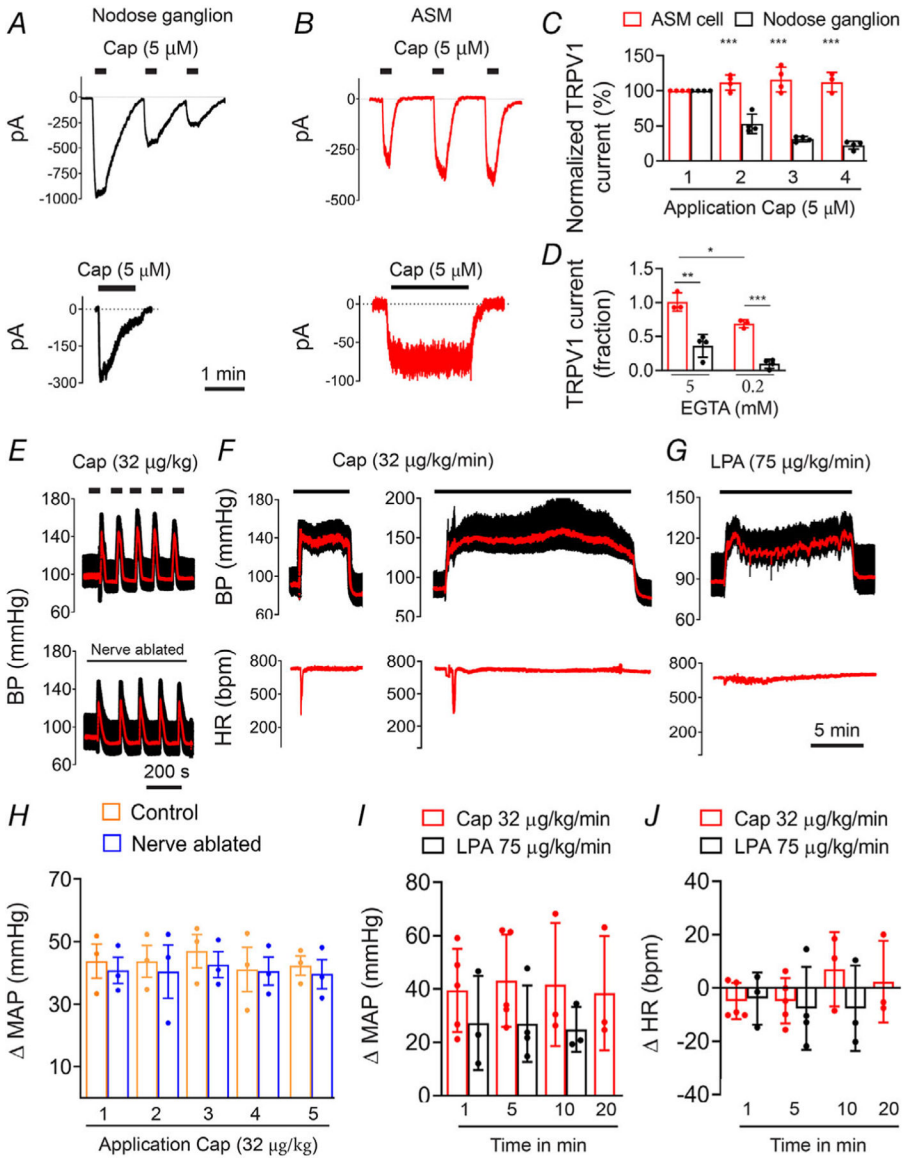

Figure 12. TRPV1 mediates persistent vasoconstriction

A and *B*, representative current traces in nodose ganglion neurons and ASM cells in response to repetitive or sustained application of capsaicin (holding potential, −50 mV). *C*, mean normalized peak current evoked by repeated capsaicin treatment in ASM cells ($n = 5$) or neurons ($n = 4$) (unpaired *t* test, $***P < 0.001$, neurons *versus* ASM cells). *D*, mean current (fraction of initial current) after 90 s application of capsaicin in ASM cells ($n = 3$) and nodose neurons ($n = 4$) measured with either low (0.2 mM) or high (5 mM) cytoplasmic EGTA (unpaired *t* test, $***P = 7.19 \times 10^{-5}$, $**P = 0.0028$,$*P = 0.0188$). *E–G*, representative BP traces in response to bolus or continuous infusion of capsaicin or LPA. *H–J*, mean changes in BP and heart rate (HR) in response to repeated or continuous administration of capsaicin ($n = 5$) or LPA ($n = 3$).

Table 1.

Artery nomenclature for Fig. 6G

(1) Superficial temporal	(16) Profunda brachii	Arteries in inset
(2) Facial	(17) Ulnar collateral	(1) Vertebral
(3) External carotid	(18) Radial branches	(2) Basilar
(4) Internal carotid	(19) Coronary	(3) Superior cerebellar
(5) Common carotid	(20) Intercostal	(4) Hypophyseal portal
(6) Vertebral	(21) Common iliac	(5) Anterior cerebral
(7) Aortic arch	(22) Femoral	(6) Anterior communicating
(8) Subclavian	(23) Saphenous	(7) Middle cerebral
(9) Axillary	(24) Iliaco-femoral	(8) Internal carotid
(10) Brachial	(25) Superficial caudal epigastric	(9) Posterior cerebral
(11) Medial	(26) Medial proximal genicular	(10) Pontine
(12) Radial	(27) Popliteal	(11) Anterior inferior cerebellar
(13) Internal mammary	(28) Proximal caudal femoral	(12) Anterior spinal
(14) Lateral thoracic	(29) Gracilis	
(15) Subscapular	(30) Median coccygeal	